

**PREDICTION OF GAS-HYDRATE FORMATION CONDITIONS IN
PRODUCTION AND SURFACE FACILITIES**

A Thesis

by

SHARAREH AMERIPOUR

Submitted to the Office of Graduate Studies of
Texas A&M University
in partial fulfillment of the requirements for the degree of

MASTER OF SCIENCE

August 2005

Major Subject: Petroleum Engineering

**PREDICTION OF GAS-HYDRATE FORMATION CONDITIONS IN
PRODUCTION AND SURFACE FACILITIES**

A Thesis

by

SHARAREH AMERIPOUR

Submitted to the Office of Graduate Studies of
Texas A&M University
in partial fulfillment of the requirements for the degree of

MASTER OF SCIENCE

Approved by:

Chair of Committee,	Maria A. Barrufet
Committee Members,	W. John Lee
	Mahmood Amani
	Malcolm Andrews
Head of Department,	Stephen A. Holditch

August 2005

Major Subject: Petroleum Engineering

ABSTRACT

Prediction of Gas-Hydrate Formation Conditions in
Production and Surface Facilities. (August 2005)

Sharareh Ameripour,

B.S., Amirkabir University of Technology, Tehran, Iran

Chair of Advisory Committee: Dr. Maria. A. Barrufet

Gas hydrates are a well-known problem in the oil and gas industry and cost millions of dollars in production and transmission pipelines. To prevent this problem, it is important to predict the temperature and pressure under which gas hydrates will form. Of the thermodynamic models in the literature, only a couple can predict the hydrate-formation temperature or pressure for complex systems including inhibitors.

I developed two simple correlations for calculating the hydrate-formation pressure or temperature for single components or gas mixtures. These correlations are based on over 1,100 published data points of gas-hydrate formation temperatures and pressures with and without inhibitors. The data include samples ranging from pure-hydrate formers such as methane, ethane, propane, carbon dioxide and hydrogen sulfide to binary, ternary, and natural gas mixtures. I used the Statistical Analysis Software (SAS) to find the best correlations among variables such as specific gravity and pseudoreduced pressure and temperature of gas mixtures, vapor pressure and liquid viscosity of water, and concentrations of electrolytes and thermodynamic inhibitors.

These correlations are applicable to temperatures up to 90°F and pressures up to 12,000 psi. I tested the capability of the correlations for aqueous solutions containing electrolytes such as sodium, potassium, and calcium chlorides less than 20 wt% and inhibitors such as methanol less than 20 wt%, ethylene glycol, triethylene glycol, and glycerol less than 40 wt%. The results show an average absolute percentage deviation of 15.93 in pressure and an average absolute temperature difference of 2.97°F.

Portability and simplicity are other advantages of these correlations since they are applicable even with a simple calculator. The results are in excellent agreement with the experimental data in most cases and even better than the results from commercial simulators in some cases. These correlations provide guidelines to help users forecast gas-hydrate forming conditions for most systems of hydrate formers with and without inhibitors and to design remediation schemes such as:

- Increasing the operating temperature by insulating the pipelines or applying heat.
- Decreasing the operating pressure when possible.
- Adding a required amount of appropriate inhibitor to reduce the hydrate-formation temperature and/or increase the hydrate-formation pressure.

DEDICATION

To those whom I think of every moment of my life:

My parents, Hassan and Sareh

My brother and sisters, Shahram, Shoaleh, and Shohreh

My nieces and nephews, Ghazaleh, Raniya, Ala, and Ragheb

My brothers-in-law and sister-in-law, Malek, Emad, and Shayesteh

and

My beloved husband, Hassan

For their love, prayers, and encouragement

ACKNOWLEDGMENTS

I would like to express my appreciation to Dr. Maria Barrufet, the chair of my advisory committee, for her great guidance and valuable advice and assistance in my research.

I would like to thank Dr. Stephen Holditch, the department head, for his interest in this research and his support.

I appreciate Dr. John Lee, Dr. Mahmood Amani, and Dr. Malcolm Andrews for serving in my advisory committee and for their helpful comments and suggestions on the manuscript of my thesis.

My special thanks go to my dear parents and brother for their support, sacrifice, and encouragement.

TABLE OF CONTENTS

	Page
ABSTRACT	iii
DEDICATION	v
ACKNOWLEDGMENTS	vi
LIST OF TABLES	ix
LIST OF FIGURES	x
 CHAPTER	
I INTRODUCTION	1
II BACKGROUND	5
2.1 Gas Hydrate Formation	5
2.2 Hydrate Structures	5
2.3 Hydrate Phase Equilibrium	8
2.4 Gas Hydrates and Problems in the Oil and Gas Industry	10
2.5 Ways to Prevent Hydrates Formation	11
2.6 Experimental Work	12
2.7 Correlation Methods	17
2.7.1 The K-Value Method	18
2.7.2 The Gas Gravity Method	19
2.7.3 Kobayashi <i>et al.</i> Method	20
2.7.4 Hammerschmidt Method	21
2.8 Thermodynamic Methods	22
2.9 Equations of State (EOS)	27
III METHODOLOGY	30
3.1 Data Collection	30
3.2 Data Observations	32
3.3 Comments on Data	35
3.4 Regression Variables	35
3.4.1 Pseudoreduced Temperature and Pressure	35
3.4.2 Gas Specific Gravity	38
3.4.3 Water Vapor Pressure	38
3.4.4 Liquid Water Viscosity	39
3.5 Hydrate-Formation Pressure Correlation	39
3.6 Hydrate-Formation Temperature Correlation	40

CHAPTER	Page
IV	RESULTS AND DISCUSSION42
	4.1 Predicted Results versus Experimental.....42
	4.2 Comparison of Predicted Results with a Common Correlation.....48
	4.3 Comparison of Predicted Results with Calculated from PVTsim48
	4.4 Sensitivity Analysis50
V	CONCLUSIONS.....55
	5.1 Conclusions from Observations.....56
	5.2 Conclusions from Developing the Improved Correlations56
	NOMENCLATURE58
	REFERENCES60
	APPENDIX A EXPERIMENTAL DATA65
	APPENDIX B HYDRATE-FORMATION PRESSURE CALCULATION.....66
	APPENDIX C HYDRATE-FORMATION TEMPERATURE CALCULATION67
	VITA.....68

LIST OF TABLES

		Page
Table 2.1	Components may enter cavities of hydrates SI and SII	7
Table 2.2	Components may enter cavities of hydrate SH.....	7
Table 2.3	Coefficients for calculating the hydrate-formation temperature from equation 2.3	21
Table 2.4	Constants used for evaluating equation 2.7	24
Table 2.5	The A and B parameters for calculating the Langmuir constants (SI & SII)	25
Table 2.6	The A and B parameters for calculating the Langmuir constants (SH).....	26
Table 3.1	Range of different independent variables for 1,104 data points	32
Table 3.2	Effects of gas compositions on hydrate-formation pressure in systems without inhibitors	33
Table 3.3	Values of constants α and β for calculating J and K	37
Table 3.4	Range of data for developing the mixing rules	37
Table 3.5	Values of constants for hydrate-formation p and T correlations.....	41

LIST OF FIGURES

		Page
Fig. 2.1	Cavities for hydrates of SI, SII, and SH.....	6
Fig. 2.2	Phase diagram for natural gas hydrocarbons which form hydrates	9
Fig. 2.3	Formation of gas hydrate plugs a subsea hydrocarbon pipeline	11
Fig. 2.4	Experimental hydrate equilibrium conditions for the ternary mixture	14
Fig. 2.5	Experimental hydrate equilibrium conditions for the natural gas mixture	15
Fig. 2.6	Experimental hydrate equilibrium conditions for pure carbon dioxide in presence of pure water, 10.04 wt% EG, and 10 wt% methanol.....	16
Fig. 2.7	Experimental hydrate equilibrium conditions for a carbon dioxide-rich gas mixture in presence of pure water, 10.04 wt% EG, and 10 wt% NaCl.....	16
Fig. 2.8	Initial hydrate-formation estimation for natural gases based on gas gravity.....	20
Fig. 3.1	Hydrate-formation pressure for binaries of CH ₄ with iC ₄ and nC ₄	34
Fig. 4.1	Comparison of experimental and calculated values of hydrate-formation pressure	43
Fig. 4.2	Comparison of experimental and calculated values of hydrate-formation temperature	43
Fig. 4.3	Comparison of experimental and calculated results of hydrate-formation-pressure from <i>p</i> -correlation for pure methane	44
Fig. 4.4	Comparison of experimental and calculated results of hydrate-formation pressure from <i>p</i> -correlation for a natural gas with low concentration of propane and nitrogen	45

	Page
Fig. 4.5	Comparison of experimental and calculated results of hydrate-formation pressure from p -correlation for a natural gas with high concentration of propane and nitrogen45
Fig. 4.6	Comparison of experimental and calculated results of hydrate-formation temperature from T -correlation for pure methane.....46
Fig. 4.7	Comparison of experimental and calculated results of hydrate-formation temperature from T -correlation for a natural gas with low concentration of propane and nitrogen47
Fig. 4.8	Comparison of experimental and calculated results of hydrate-formation temperature from T -correlation for a natural gas with high concentration of propane and nitrogen47
Fig. 4.9	Actual differences between predicted and experimental temperatures for T -correlation and Kobayashi <i>et al.</i> correlation48
Fig. 4.10	Comparison of the calculated hydrate-formation pressure from PVTsim and p -correlation.....49
Fig. 4.11	Comparison of the calculated hydrate-formation temperature from PVTsim and T -correlation.....50
Fig. 4.12	Calculated results from PVTsim before and after adjusting the value of A for component C_1 in a large cavity of Structure II.....53
Fig. 4.13	Calculated results from PVTsim before and after adjusting the value of A for component C_2 in a large cavity of Structure I53

CHAPTER I

INTRODUCTION

Gas hydrates are ice-like crystalline structures with gas components such as methane and carbon dioxide as guest molecules entrapped into cavities formed by water molecules. Whenever a system of natural gas and water exists at specific conditions, especially at high pressure and low temperature, we expect the formation of hydrates. In the oil and gas industry, gas hydrates are a serious problem in production and gas-transmission pipelines because they plug pipelines and process equipment. By applying heat, insulating the pipelines, and using chemical additives as inhibitors, we can keep the operating conditions out of the hydrate-formation region.

The most common inhibitors are thermodynamic inhibitors such as methanol and glycols; however, produced water that contains electrolytes also has inhibiting effects. To remediate problems caused by hydrates, it is important to calculate the gas-hydrate formation temperature and pressure accurately; this is more complex when the system includes alcohols and/or electrolytes.

Hammerschmidt¹ first found that the formation of clathrate hydrates could block natural gas-transport pipelines. Since then, the oil and gas industry has been more willing to investigate the problem. My work focuses on gas-hydrate formation in three-phase equilibrium (liquid water, hydrocarbon gas, and solid hydrate) with the objectives of developing a correlation to predict the gas-hydrate formation at a given temperature, a correlation to predict the gas-hydrate formation temperature when pressure is available, and guidelines to calibrate a thermodynamic model by analyzing sensitivity to selective parameters such as temperature- dependent adsorption constant.

This thesis follows the style of *SPE Reservoir Evaluation & Engineering*.

It is not practical to measure the gas-hydrate formation pressure and temperature for every particular gas mixture. The main objective of this research is to develop correlations to predict these conditions with the least average absolute error. To approach that, I used over 1,100 experimental points²⁻¹⁸ among over 1,400 points gathered from published literature from 1940 till 2004. The removed points are those that either presented off-trend hydrate formation curves or those that contained high concentrations of inhibitors. The data include samples ranging from single-hydrate formers such as methane, carbon dioxide, ethane, propane, and hydrogen sulfide to binary, ternary, and natural gases in the presence of pure water, electrolytes and/or alcohols. Using the Statistical Analysis Software (SAS),¹⁹ I applied a regression model to find the best correlations among the variables, such as specific gravity and pseudoreduced pressure and temperature of gas mixtures, vapor pressure and liquid viscosity of water, and concentrations of electrolytes and thermodynamic inhibitors.

I developed two correlations that are able to predict the hydrate formation pressure for a given temperature or hydrate formation temperature for a given pressure for a single or multicomponent gas mixture with and without electrolytes and/or thermodynamic inhibitors. These correlations are applicable to a range of temperatures up to 90°F and pressures up to 12,000 psi. The capability of the correlations has been tested for aqueous solutions containing electrolytes such as sodium, potassium, and calcium chlorides lower than 20 wt% and inhibitors such as methanol lower than 20 wt%, ethylene glycol (EG), triethylene glycol (TEG), and glycerol (GL) lower than 40 wt% since the use of higher amount of these inhibitors is not practical because is very costly. The results show an average absolute percentage deviation of 15.93 in pressure and an average absolute temperature difference of 2.97°F.

To make the correlations easy to use, I programmed them with Visual Basic. By giving the gas compositions, the inhibitor concentrations, and either temperature or pressure of the system, a user can calculate the hydrate-formation pressure or temperature as quickly as clicking a key.

Gas-hydrate plugging is a challenging and costly problem in gas-gathering systems and transmission pipelines. Several models have been published in the literature, but not all of them are applicable for a complex system including gas-hydrate formers and mixed inhibitors. My correlations will provide guidelines to help the user forecast the gas-hydrate formation pressure or temperature for a pure or mixed gas with and without inhibitors at a given temperature or pressure. They will also be able to determine the most appropriate inhibitor for the given system without the need of doing costly and time-consuming experimental measurements. The advantage of these correlations is that they will not require sophisticated calculations or a computer; instead, they are applicable even with a simple calculator. The disadvantage of these correlations is that they may not be appropriate in some cases with high concentrations of inhibitors.

Chapter II of this thesis gives general information about the phase equilibrium of forming hydrates and different types of determined hydrate structures, problems that they may cause in the oil and gas industry, and solutions that may prevent their formation. This chapter also reviews the literature in terms of experimental works, the available correlation methods, and finally the basis of calculating the hydrate-formation conditions from thermodynamic models. Chapter III explains the methodology for developing the proposed correlations including my observations from the experimental data, the regression variables that I used in this work, and an introduction to the new correlations that improved the estimation of hydrate-formation conditions in systems with and without inhibitors. Chapter IV includes the results of the regression models for both correlations; it also shows the comparisons of calculated results from this work with the experimental data, with a commonly used correlation, and with the results predicted by the PVTsim²⁰ simulator for several gas systems. Chapter V contains the conclusions from this work and from data observations.

There are three appendixes that come separately in Excel files. Appendix A includes the experimental data gathered and used in this work. Appendix B contains a Visual Basic program that calculates hydrate-formation pressure at a given temperature and Appendix

C is a Visual Basic program that calculates hydrate-formation temperature at a given pressure.

CHAPTER II

BACKGROUND

2.1 Gas Hydrate Formation

Gas hydrates are nonstoichiometric compounds formed from mixtures of water and gas molecules under suitable pressures and temperatures. Gas molecules with adequate size become guest molecules entrapped in the cavities of cages formed by water molecules acting as host molecules. Hydrates are also called clathrates, which in Latin means, “cage.” When a minimum number of cavities are occupied by the gas molecules, the crystalline structure stabilizes and solid gas hydrates may form at temperatures above the water freezing point. Most light molecules such as methane, ethane, propane, isobutane, normal butane, nitrogen, carbon dioxide, and hydrogen sulfide will form hydrates under specific conditions of pressure and temperature; however, several heavy hydrocarbons such as benzene, cyclopentane, cyclohexane, methylcyclopentane, methylcyclohexane, isopentane and 2,3-dimethylbutane have been recently identified as hydrate formers.²¹

2.2 Hydrate Structures

Von Stackelberg and Muller²² studied the hydrate structure using X-ray diffraction methods. Their work along with works by Classen^{23, 24} identified two hydrate structures, Structure I (SI) and Structure II (SII) that each has two types of cavities. The SI hydrates consist of 46 water molecules per eight cavities, two small spherical cavities with 12 pentagonal faces (5^{12}) and six large oblate cavities with two hexagonal faces and 12 pentagonal faces ($5^{12}6^2$).²⁵ The SII hydrates consist of 136 water molecules per 32 cavities, 16 small cavities with 12 pentagonal faces (5^{12}) and eight large cavities with 12 pentagonal and four hexagonal faces ($5^{12}6^4$), all in a spherical shape. **Fig. 2.1** shows these cavities.

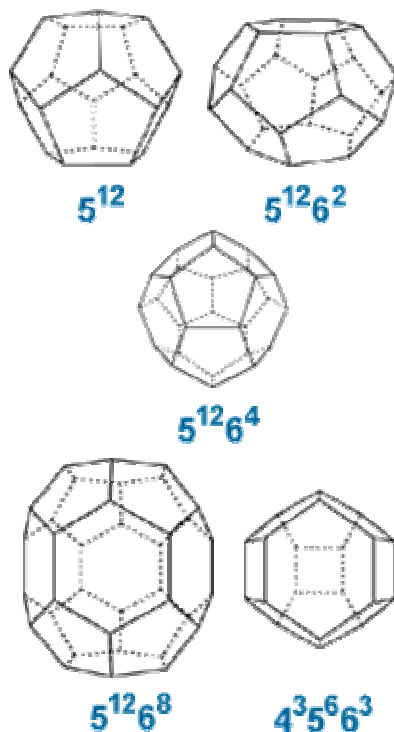


Fig. 2.1—Cavities for hydrates of SI, SII, and SH.²⁵

From 1959 to 1967, Jeffrey, McMullan, and Mak²⁶⁻²⁸ studied crystallography on hydrates SI and SII. A summary of their experience showed that hydrates are “clathrates”. It is well known that small gas molecules such as CH_4 , C_2H_6 , and CO_2 form hydrate Structure I, but gas molecules with larger size such as C_3H_8 and $i\text{-C}_4\text{H}_{10}$ form hydrate Structure II. However, some of the small gas molecules like Ar and Kr form both hydrate structures.⁷

Table 2.1 and **Table 2.2** show the molecules that may enter hydrate cavities.

Component	Structure I		Structure II	
	Small Cavities	Large Cavities	Small Cavities	Large Cavities
C ₁	+	+	+	+
C ₂	–	+	–	+
C ₃	–	–	–	+
nC ₄	–	–	–	+
iC ₄	–	–	–	+
CO ₂	+	+	+	+
N ₂	+	+	+	+
H ₂ S	+	+	+	+
O ₂	+	+	+	+
Ar	+	+	+	+
2,2 Dimethylpropane	–	–	–	+
Cyclopropane	–	–	–	+
Cyclohexane	–	–	–	+
C ₆ H ₆	–	–	–	+

Component	Small/Medium Cavities	Huge Cavities
C ₁	+	–
N ₂	+	–
iC ₅	–	+
Neohexane	–	+
2,3-Dimethylbutane	–	+
2,2,3-Trimethylbutane	–	+
3,3-Dimethylpentane	–	+
Methylcyclopentane	–	+
1,2- Dimethylcyclohexane	–	+
Cis-1,2- Dimethylcyclohexane	–	+
Ethylcyclopentane	–	+
Cyclooctane	–	+

Ripmeester *et al.*³⁰ discovered a third type of hydrate structure (Structure H). The formation of hydrate SH requires both small and large molecules to be stabilized. The hydrates with SH contain 34 water molecules per six cavities, three cavities formed by 12 pentagonal (5^{12}), two cavities formed by three square, six pentagonal, and three hexagonal faces ($4^3 5^6 6^3$), and one large cavity formed by 12 pentagonal and eight hexagonal faces ($5^{12} 6^8$).²⁵

Hydrate formation of type sH requires large gas molecules such as methylcyclopentane, which are generally found in gas-condensate and oil systems. My work focuses on Structure I and mostly Structure II, which are basically formed by natural gas. The structure type of hydrates does not affect the magnitude of flow blockage in wells or pipelines; however, most of the thermodynamic models consider the effects of the hydrate structures and the size of their cavities as we will see in Section 3.3. In this work, since none of the variables represent the hydrate structures in the regression model, the structure of hydrates has not been directly involved in the development of the new correlations; however, because components with different sizes form different types of hydrate structures, we assume that our correlations have accounted for the hydrate structure in their specific gravity and pseudoreduced temperature and pressure variables.

Tohidi *et al.* measured the SH equilibrium data for benzene, cyclohexane, cyclopentane, and neopentane.^{31, 32} Becke *et al.*³³ measured SH for methane+methylcyclohexane, and Ostergaard *et al.*³⁴ for isopentane and 2,2-dimethylpentane in their binaries and ternaries with methane and/or nitrogen. Mehta and Sloan³⁵ provided an overview of the state-of-the-art on SH hydrates with an emphasis on its implications for the petroleum industry.

2.3 Hydrate Phase Equilibrium

Fig. 2.2^{2,36} shows the hydrate equilibrium curve ($I-H-V$), (L_W-H-V), (L_W-H-L_{HC}) for several components. The letters H , I , V , L_W , and L_{HC} represent hydrate, ice, hydrocarbon vapor, liquid water, and hydrocarbon liquid respectively. The lower quadruple point, Q_I indicates the point at which the four-phase ice, liquid water, hydrocarbon vapor and

hydrate ($I-L_W-H-V$) are in equilibrium. The temperature at this point approximates the ice point.

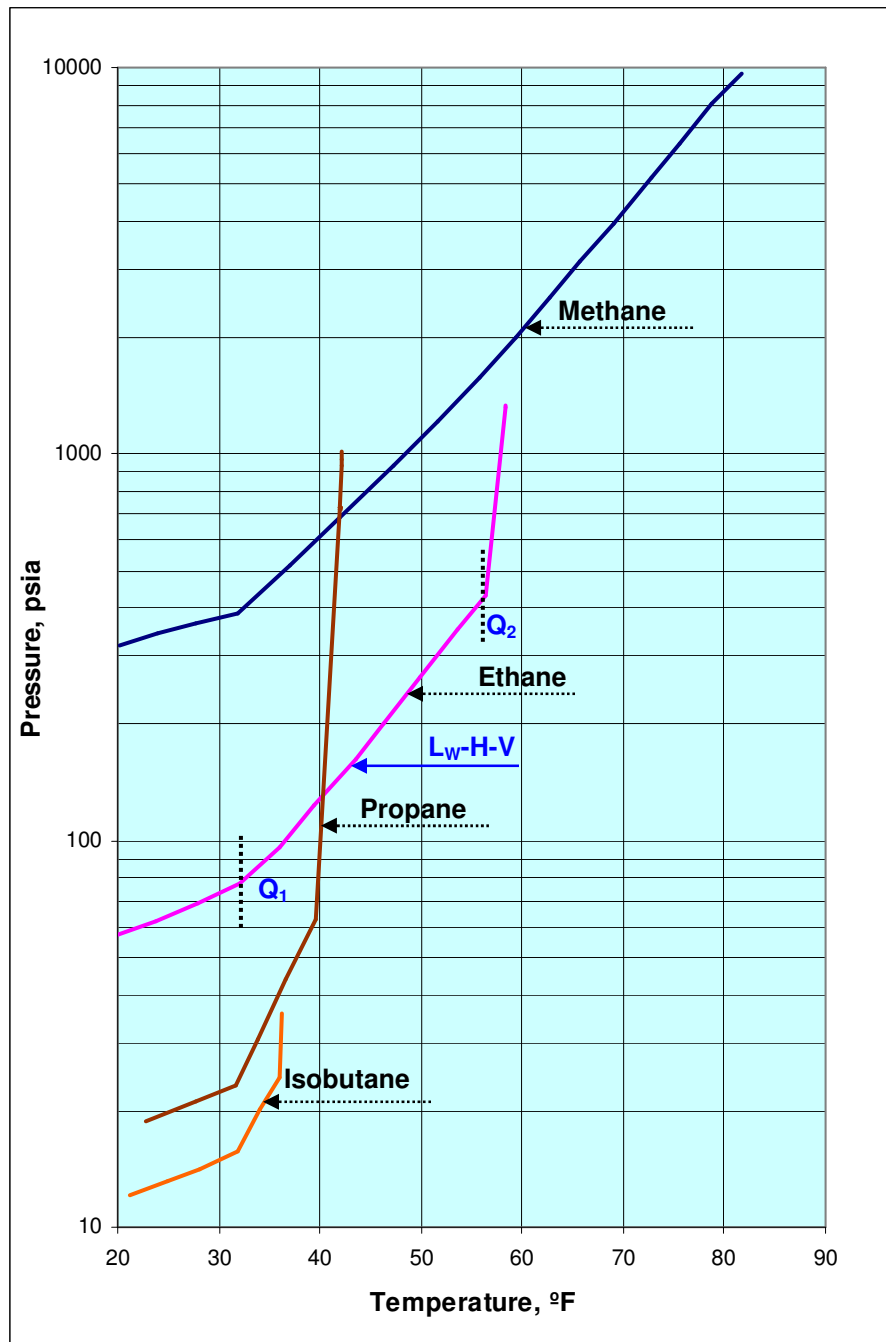


Fig. 2.2—Phase diagram for natural gas hydrocarbons which form hydrates (after McCain).³⁶

The point Q_2 is the upper quadruple point at which the four-phase water liquid, hydrocarbon liquid, hydrocarbon vapor, and hydrate ($L_W-L_{HC}-V-H$) are in equilibrium. The pressures and temperatures at the Q_1Q_2 line represent the conditions that three-phase liquid water, hydrocarbon vapor and hydrate are in equilibrium. Therefore, at the right side of this line no hydrates form; however, hydrates begin to form at this line and become more stable at a higher pressure and/or lower temperature. Since our objective in this work is to predict the incipient hydrate-formation pressure or temperature, all the experimental data gathered and used in developing the new correlations are those that represent the three-phase equilibrium line (L_W-H-V).

2.4 Gas Hydrates and Problems in the Oil and Gas Industry

Hammerschmidt¹ determined that natural gas hydrates could block the gas transmission pipelines sometimes at temperature above the water freezing point. This discovery highlighted the importance of hydrates to the oil and gas industry and was an introduction to the modern research era.

Gas hydrates are a very costly problem in petroleum exploration and production operations. Hydrate clathrates can plug gas gathering systems and transmission pipelines subsea and on the surface. In offshore explorations, the main concern is the multiphase transfer lines from the wellhead to the production platform where low seabed temperatures and high operation pressures promote the formation of gas hydrates. **Fig. 2.3** shows plugging of a subsea hydrocarbon pipeline because of hydrate formation.



Fig. 2.3—Formation of gas hydrate plugs a subsea hydrocarbon pipeline.²⁵

2.5 Ways to Prevent Hydrate Formation

The following are the thermodynamic ways to prevent the hydrate formation:

1. Reducing the water concentration from the system.
2. Operating at temperatures above the hydrate-formation temperature for a given pressure by insulating the pipelines or applying heat.
3. Operating at pressures below the hydrate-formation pressure for a fixed temperature.
4. Adding inhibitors such as salts, methanol, and glycols to inhibit the hydrate-formation conditions and shift the equilibrium curve to higher pressure and lower temperature.

Inhibitors are added into processing lines to inhibit the formation of hydrates. There are two kinds of inhibitors: thermodynamic inhibitors and low-dosage inhibitors.³⁷ The thermodynamic inhibitors have been used for long time in the industry and act as

antifreeze. The low-dosage inhibitors have recently been developed and their usage modifies the rheology of the system rather than changing its thermodynamic states. These inhibitors work at low concentrations, lower than or equal to 1 wt%; therefore, the use of this technique reduces the environmental concerns and since no regeneration units are required, it results in reduction of capital cost. The low-dosage inhibitors are divided into kinetic inhibitors and antiagglomerants. The kinetic inhibitors are commonly water-soluble polymers delay the nucleation and growth of hydrate crystals, while the anti-agglomerants are usually surfactants and miscible in both hydrocarbon and water, so they impede the agglomeration of hydrate crystals for a period of time without interfering with crystal formation.

2.6 Experimental Work

Ng and Robinson³⁸ obtained experimental data on initial hydrate formation conditions for the nitrogen-propane-water system in the L_W-H-V , $L_W-L_{HC}-H$, and $L_W-L_{HC}-H-V$ regions, where L_W is the water-rich liquid phase, L_{HC} is the hydrocarbon rich liquid phase, H is the hydrate and V is the vapor phase. The measurements covered a range of temperatures from about 275 to 293°K and pressures from about 0.3 to 17 MPa with the concentrations of propane from 0.94 to 75 mol% in the gas phase for the L_W-H-V region, and from 83.1 to 99 mole percent in the condensed liquid phase for the $L_W-L_{HC}-H$ region. Ng and Robinson used these experimental data to fit a binary interaction parameter to predict hydrate formation in systems containing nitrogen and propane. Based on their proposed method, Ng and Robinson³⁹ found the best value of the interaction parameter for nitrogen-propane mixtures to be 1.03, which is much higher than usual values (-0.5, 0.5). They reported that using this parameter will reduce the absolute average error from 15.3 to 5.7% for predicting the hydrate-formation pressures at a given temperature in the L_W-H-V region. The importance of this parameter in this system becomes more significant as the concentration of propane in the gas phase becomes higher.

Most of the experimental studies on gas hydrates have investigated systems in the presence of pure water but have lacked information on hydrate inhibition. Ng and Robinson¹¹ studied the hydrate-forming conditions for pure gases, including methane,

ethane, propane, carbon dioxide, and hydrogen sulfide, and for selected binary mixtures in the presence of solutions up to 20 wt% methanol. This study was carried out in both the L_W-H-V and the L_W-H-L_{HC} regions for all the mentioned hydrate formers, but for methane only in the L_W-H-V region. The experimental measurements covered a range of pressures from about 0.8 to 20 MPa, temperature from -10 to 17°C, and concentration of methanol from 5 to 20 wt%. Ng and Robinson¹¹ used the results of these measurements to compare with the calculated values from the Hammerschmidt equation²⁹ as we will see in Section 2.7.4. This equation calculates the difference between the temperature of a system in the presence of water and the temperature of system in an inhibitor solution. The difference between experimental and calculated hydrate-temperature depression from their experiment was less than 1°C for CH₄, C₂H₆, and C₃H₈ in the gaseous region and more than 1°C in the region of liquid. This difference was more than 1°C for CO₂ in gaseous and liquid regions. The results show that the Hammerschmidt equation overestimates the hydrate-temperature depression for H₂S in the gaseous region but provides estimates for this component than the other components in the liquid region.

Inhibitors such as ethylene glycol, methanol, and electrolytes inhibit hydrate formation. It is important to determine the inhibition effects of these additives to avoid hydrate formation and select the best inhibitor for a given system and operating conditions. Bishnoi and Dholabhai⁴⁰ obtained experimental hydrate equilibrium conditions for propane hydrate with single and mixed electrolytes. Their work included electrolytes such as NaCl, KCl, and CaCl₂ at pressure and temperature ranges of 133 to 500 KPa and 263 to 276°K. The results of this work show that for the same concentrations of electrolytes (5 and 10 wt% in this case), sodium chloride has a greater inhibition effect than potassium and calcium chlorides.

Bishnoi and Dholabhai⁵ obtained the hydrate-equilibrium conditions for a ternary mixture of methane (78 mol%), propane (2 mol%) and carbon dioxide (20 mol%) and a natural gas mixture in pure water and solutions containing methanol and electrolytes for a temperature range of 274 to 291°K and a pressure range of 1.5 to 10.1 MPa. They observed systems that contain the same total wt% of the inhibitor, for example systems

with 10 wt% of either methanol or sodium chloride and 20 wt% of either methanol or sodium chloride, 15 wt% of methanol + 5 wt% of sodium chloride, and 5 wt% of methanol + 15 wt% of sodium chloride. For a given pressure, they reported that the incipient hydrate-equilibrium conditions for such systems are close to each other, within 3 to 5°C (**Figs. 2.4 and 2.5**); one can also conclude from these two figures that sodium chloride has higher inhibition potential than methanol with the same wt%, a result is more pronounced at higher pressures. Even in the presence of mixed inhibitors, the inhibitor with a higher wt% of sodium chloride is more effective than the one with higher wt% of methanol.

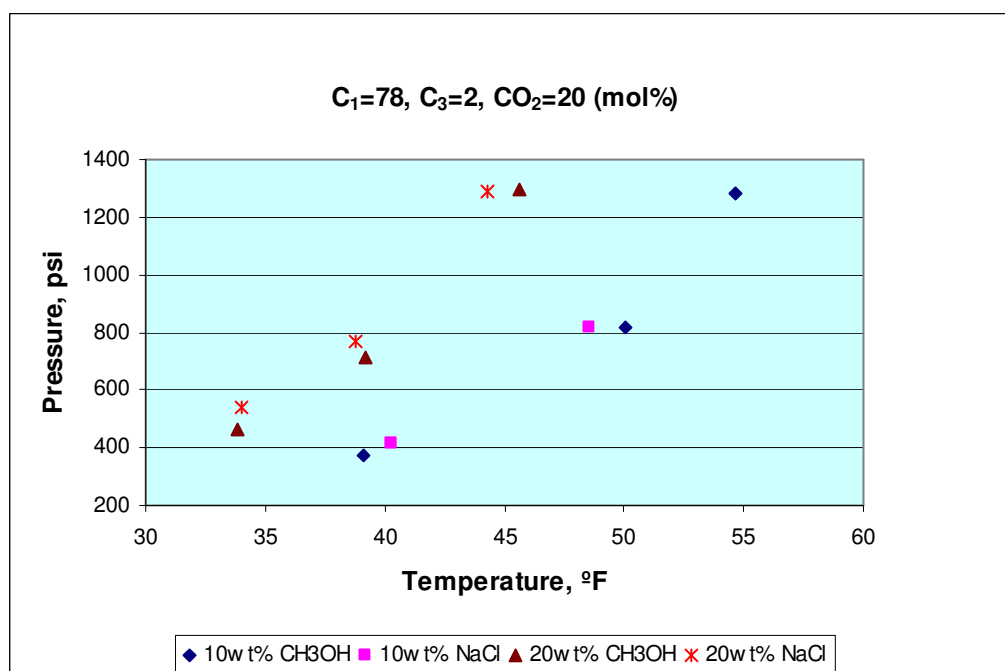


Fig. 2.4—Experimental hydrate equilibrium conditions for the ternary mixture.⁵

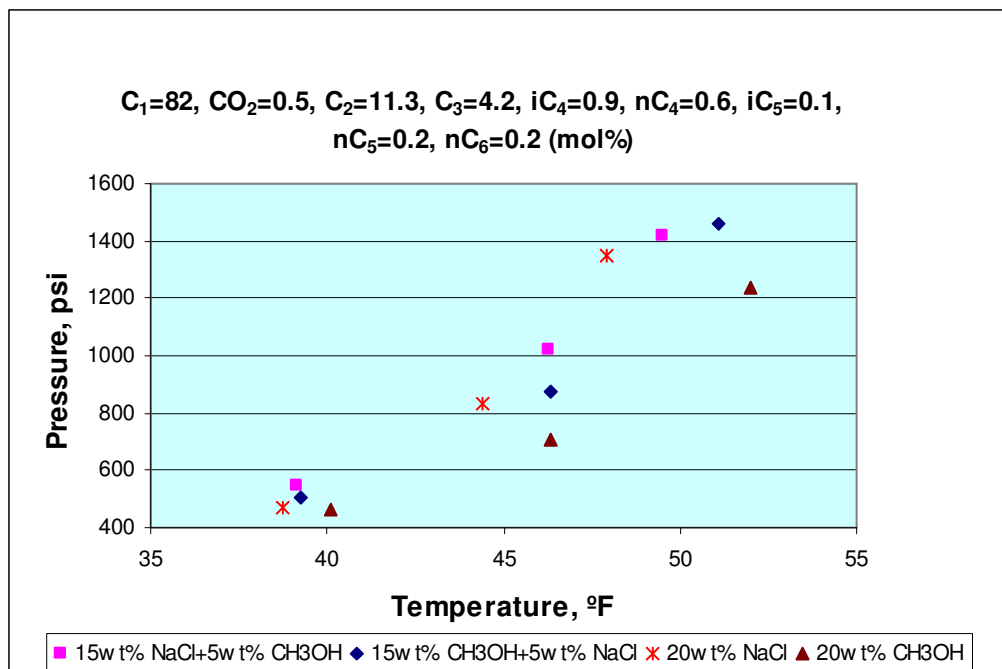


Fig. 2.5—Experimental hydrate equilibrium conditions for the natural gas mixture.⁵

Fan *et al.*¹⁸ measured the hydrate-formation pressures of pure carbon dioxide in water, 10 wt% methanol, and 10 wt% ethylene glycol (EG) solutions and concluded that the inhibition effect of EG is inferior to that of methanol, as indicated in **Fig. 2.6**. To compare the inhibition effects, they also determined the hydrate formation data for a carbon dioxide-rich quaternary gas mixture containing 88.53 mol% CO₂, 6.83 mol% CH₄, 4.26 mol% N₂, and 0.38 mol% C₂H₆ in presence of 10 wt% EG and 10 wt% NaCl. The results show that the inhibition of EG is less effective (**Fig. 2.7**).

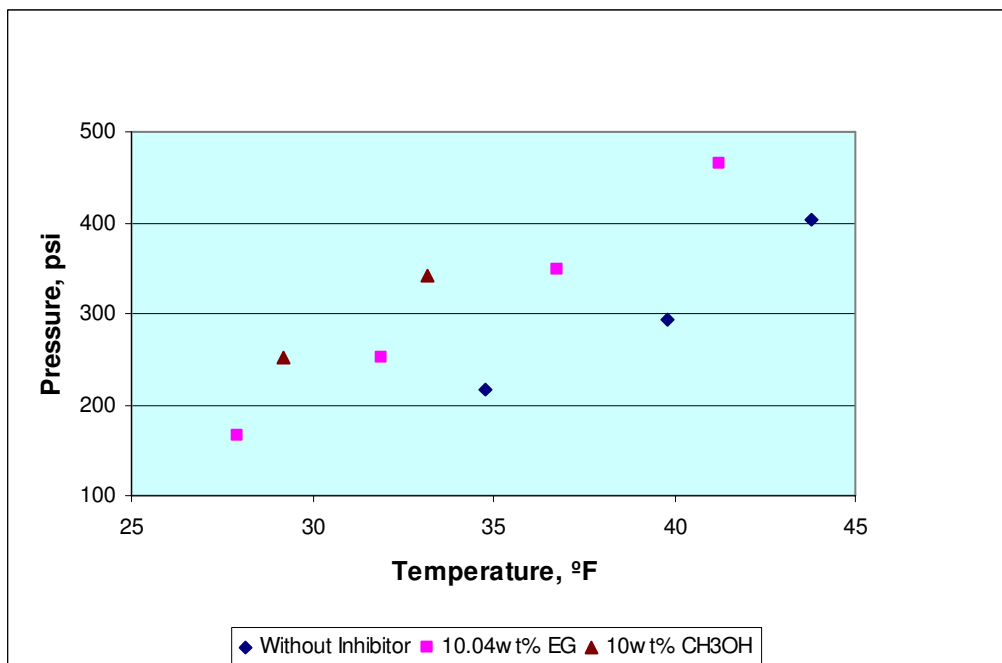


Fig. 2.6—Experimental hydrate equilibrium conditions for pure carbon dioxide in presence of pure water, 10.04 wt% EG, and 10 wt% methanol.¹⁸

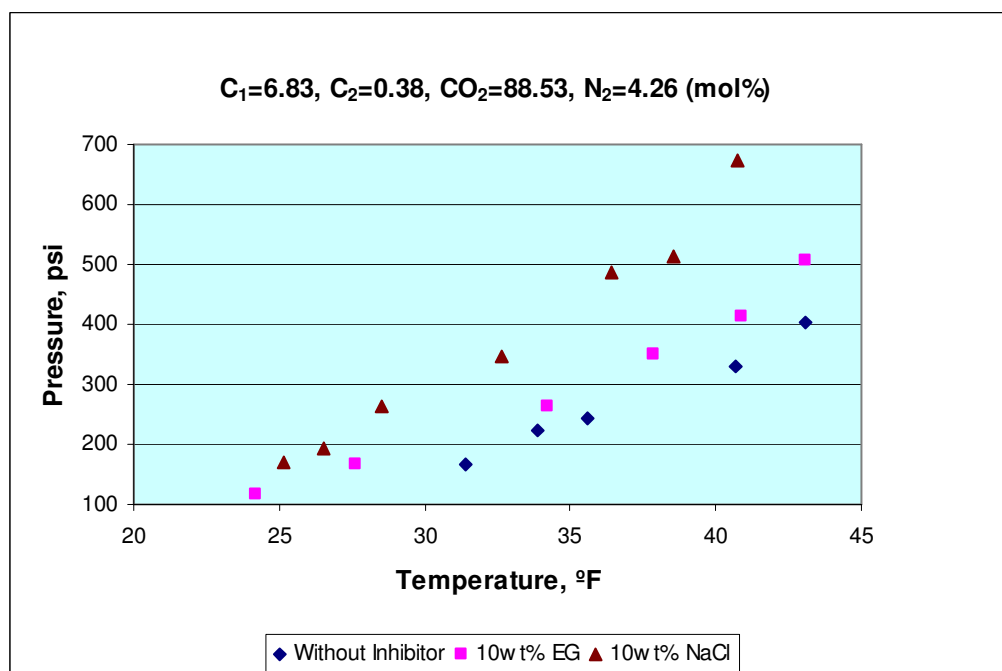


Fig. 2.7—Experimental hydrate equilibrium conditions for a carbon dioxide-rich gas mixture in presence of pure water, 10.04 wt% EG, and 10 wt% NaCl.¹⁸

In another work, Ma *et al.*¹⁶ determined the initial hydrate formation data of pure ethylene, five binary gas mixtures of methane/ethylene, and four binary gas mixtures of methane/propylene for temperatures of 273.7 to 287.2°K and pressures of 0.53 to 6.6 MPa. The ethylene and propylene contents in the mixtures range from 7.13 to 100 mol% and 0.66 to 71.96 mol%. Their work showed that the model developed by Chen and Guo represented the measured data; however, my conclusion from the experimental results is that hydrates could form at higher pressure as the concentration of methane increased in the mixture. This means that at the same temperature, the lighter the gas specific gravity of the hydrate former, the higher the pressure at which hydrates form, as indicated in the literature.³⁶

Sometimes the processed water in pipelines contains electrolytes which also act as inhibitors. To establish the effect of mixtures of inhibitors on the locus of the three-phase equilibrium curve, Jager, Peters, and Sloan¹² measured data on eight different mixtures of the quaternary system of methane/water/methanol/sodium chloride. They reported 16 data points at a relative concentration of 2 and 4 mol% sodium chloride combined with 10, 20, 30 and 40 wt% of methanol. Using two different experimental methods, they measured the incipient hydrate values for pressures from 2 to 14 MPa in a Cailletet apparatus and from 2 to 70 MPa in a Raman spectroscopy, which had not been used before to measure hydrate data in complex systems. The results from the two apparatus at 10 MPa are consistent within 0.3 to 1°K. They compared the data collected in their work with literature data for the ternary systems of methane/water/sodium chloride and methane/water/methanol and concluded that the mixtures of inhibitors (sodium chloride + methanol in this case) have a larger inhibition effect than the sum of the inhibition effect by each inhibitor; therefore, thermodynamic models must consider the interaction between electrolytes and methanol to predict hydrate inhibition correctly.

2.7 Correlation Methods

It is well known that Davy discovered hydrates in 1810 and his discovery was confirmed by Faraday in 1823;² however, hydrates became a subject of study in the oil and gas industry after Hammerschmidt¹ found that hydrates could plug natural gas pipelines and

process equipment. After Hammerschmidt's discovery of hydrate blocking in 1934, Katz *et al.*⁴¹ started an experimental study on hydrates. Because it was impractical to measure the hydrate formation pressure and temperature for every gas compositions they estimated the hydrate formation conditions for natural gases using two approaches. Since these models were developed before discovery of the structure H hydrate, they are only able to predict the hydrate formation conditions for light hydrate formers that form Structure I and Structure II hydrates but not Structure H.

2.7.1 The *K*-Value Method

In the first approach, Wilcox *et al.*^{42, 43} initiated the *K*-Value method based on distribution coefficients (K_i values) for components on a water-free basis. In the finalized method, they determined that hydrates were a solid solution that might be treated similarly to an ideal liquid solution and defined the value as the vapor/solid equilibrium ratio of a component in L_W-H-V equilibrium by the following equation:

$$K_i^{vs} = y_i / s_i, \dots \dots \dots (2.1)$$

where y_i = mol fraction of component i in the vapor phase and s_i = mol fraction of component i in the solid phase. Therefore, similar to the dewpoint calculation in vapor/liquid equilibria, the *K*-Value charts are used to calculate the hydrate formation temperature or pressure of three-phase (L_W-H-V) solution in a manner that satisfies the following equation:

$$\sum_{i=1}^n \frac{y_i}{K_i^{vs}} = 1 \dots \dots \dots (2.2)$$

The *K*-Value method was generated before determination of the hydrate-crystal structure and was improved by Katz and co-workers. The *K*-Value charts were generated for methane, ethane, propane, butane, carbon dioxide, hydrogen sulfide, and nitrogen. Having the *K*-Value of every component in the mixture at three-phase (L_W-H-V)

equilibrium, users could determine the hydrate-formation pressure at a given temperature or vice versa. This method is limited to the hydrate-formation pressures up to 4,000 psia for methane, ethane, and propane; up to 2,000 psia for isobutane and hydrogen sulfide; and up to 1,000 psia for carbon dioxide.

2.7.2 The Gas Gravity Method

In a different approach, Katz and his students^{2, 43} generated the gas-gravity plot (**Fig. 2.8**) that relates the hydrate pressure and temperature with the specific gravity (gas molecular weight divided by that of air) of natural gases, not including non-hydrocarbons. This plot was generated from limited experimental data from Deaton and Frost, Wilcox *et al.*, Kobayashi and Katz and significant calculations based on the *K*-Value method.²

This method is simple and may be used for an initial estimation of hydrate formation conditions. Elgibaly and Elkamel⁴⁴ have mentioned in their paper that Sloan showed in a statistical analysis report that this method is not accurate and that the calculated pressure for the same gas gravity with different mixtures may result in 50% error. Since method considers only the gas gravity of the components, if two components have equal molecular weights such as butane and isobutene, the method may estimate the same hydrate-formation temperature or pressure, although they should be different in reality. I have shown on page 34 the experimental data for two binary gases with the same gas specific gravity in the same range of temperature that form hydrates at a very different range of pressure.

For three-phase (L_W - H - V) conditions, Kobayashi *et al.*⁴³ developed an empirical equation that predicts the hydrate temperatures at given pressures for systems including only hydrocarbons in limited range of temperatures, pressures, and gas specific gravities. I have compared the calculated results from Kobayashi *et al.* with the calculated results from our new correlation in Chapter IV.

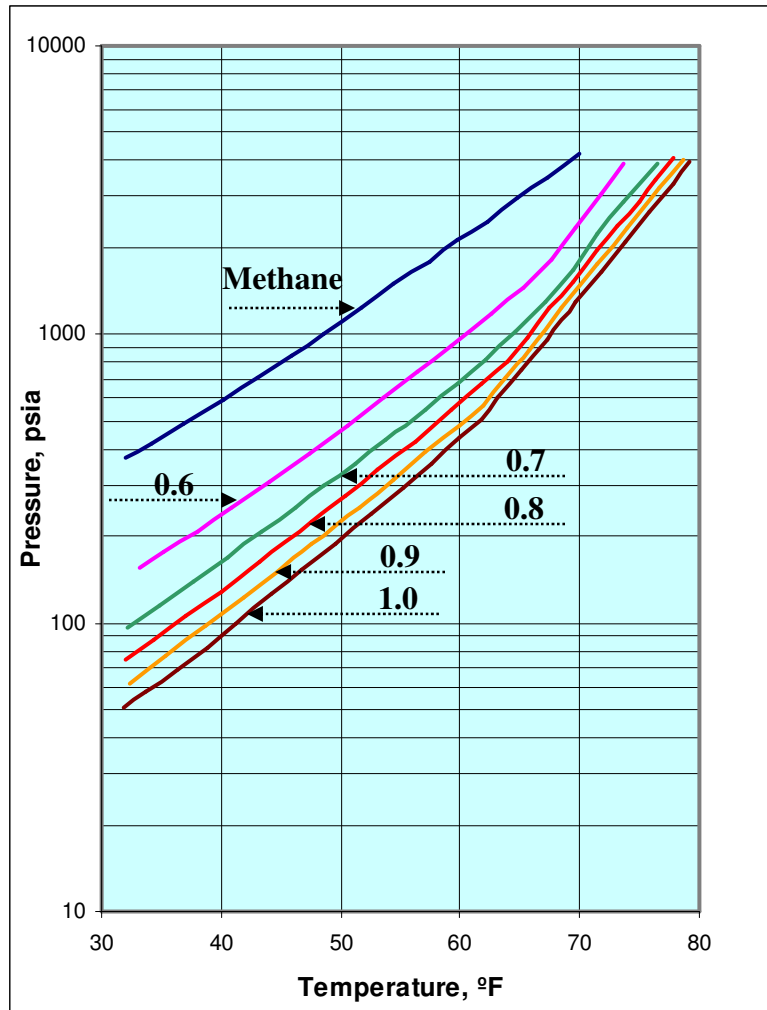


Fig. 2.8—Initial hydrate-formation estimation for natural gases based on gas gravity (after McCain).³⁶

2.7.3 Kobayashi *et al.* Method

Kobayashi *et al.*⁴³ developed Eq. 2.3 on the basis of the gas-gravity plot to estimate the hydrate-formation temperature at a given pressure. The reference did not give the units for temperature and pressure; therefore, I had to try different combinations of units for temperature and pressure to find the units that best predicted the temperature of the experimental data. I found that by having pressure in bar and temperature in °C, the Kobayashi *et al.* correlation would have the best results with experimental data.

$$T = 1/[c_1 + c_2(\ln p) + c_3(\ln \gamma) + c_4(\ln p)^2 + c_5(\ln p)(\ln \gamma) + c_6(\ln \gamma)^2 + c_7(\ln p)^3 + c_8(\ln \gamma)(\ln p)^2 + c_9(\ln \gamma)^2(\ln p) + c_{10}(\ln \gamma)^3 + c_{11}(\ln p)^4 + c_{12}(\ln \gamma)(\ln p)^3 + c_{13}(\ln \gamma)^2(\ln p)^2 + c_{14}(\ln \gamma)^3(\ln p) + c_{15}(\ln \gamma)^4] \dots\dots\dots (2.3)$$

This method is a regression method that correlates temperature (T), pressure (p), and gas specific gravity (γ) at three-phase equilibrium. The equation is applicable in the temperature range of 34 to 60°F, the pressure range of 65 to 1,500 psia, and gas gravity range from 0.552 to 0.9. The three-phase condition was fit only for hydrocarbons and not gases containing CO₂ and H₂S. **Table 2.3** shows the coefficients for this correlation.

$c_1 = 2.7707715 \times 10^{-3}$	$c_2 = -2.782238 \times 10^{-3}$	$c_3 = -5.649288 \times 10^{-4}$
$c_4 = 1.298593 \times 10^{-3}$	$c_5 = 1.407119 \times 10^{-3}$	$c_6 = 1.785744 \times 10^{-4}$
$c_7 = 1.130284 \times 10^{-3}$	$c_8 = 5.9728235 \times 10^{-4}$	$c_9 = -2.3279181 \times 10^{-4}$
$c_{10} = -2.6840758 \times 10^{-5}$	$c_{11} = 4.6610555 \times 10^{-3}$	$c_{12} = 5.5542412 \times 10^{-4}$
$c_{13} = -1.4727765 \times 10^{-5}$	$c_{14} = 1.3938082 \times 10^{-5}$	$c_{15} = 1.4885010 \times 10^{-6}$

2.7.4 Hammerschmidt Method

Hammerschmidt^{2, 29} proposed an empirical equation to calculate the effect of alcohols on hydrate formation; however, his work includes no experimental data on the effect of inhibitors added to the water and it cannot be used unless the hydrate-formation conditions in the presence of pure water have been determined.

$$\Delta T = \frac{k_j x_j}{(100 \times M_j - x_j \times M_j)} \dots\dots\dots (2.4)$$

The following are the values of constant k for different inhibitors²⁹:

$k = 2,335$ for methanol.

$k = 2,700$ for ethylene glycol.

$k = 5,400$ for triethylene glycol.

ΔT is the difference in °C between the hydrate-formation temperatures in the presence of pure water and in a methanol solution, M_j is the molecular weight of the inhibitor j , and x_j is the concentration of inhibitor j in weight percent.

2.8 Thermodynamic Methods

Parrish and Prausnitz⁴⁵ developed the first thermodynamic model for calculating hydrate-formation conditions based on a statistical method by van der Waals and Platteeuw. Du and Guo¹⁰ developed a model to predict the hydrate-formation conditions for systems including alcohol solutions. The model by Javanmardi and Moshfeghian⁴ can predict the hydrate-formation conditions for systems including electrolyte solutions. If the system includes electrolytes and alcohol, the model by Nasrifar *et al.*⁸ and the model by Nasrifar and Moshfeghian³ can be used to predict the hydrate formation conditions.

The transformation from a pure-water state to a hydrate state can be considered in two steps:

- 1) pure water (aq) \rightarrow empty hydrate lattice (β), and
- 2) empty hydrate lattice (β) \rightarrow filled hydrate lattice (H),

where aq indicates the state of pure water, H the filled hydrate lattice, and β indicates the empty hydrate lattice, which is hypothetical but used to facilitate the hydrate calculations.

In a system at three-phase equilibrium of vapor/hydrate/aqueous, the chemical potential of water in hydrate and aqueous phases is equal and can be expressed as:

$$\mu^{aq} = \mu^H \dots\dots\dots (2.5)$$

If μ^β is the indication of the hypothetical empty-hydrate phase, then Eq. 2.5 can be written as:

$$\Delta\mu^{aq} = \Delta\mu^H, \dots\dots\dots (2.6)$$

where $\Delta\mu^{aq} = \mu^\beta - \mu^{aq}$ and $\Delta\mu^H = \mu^\beta - \mu^H$.

The term of $\Delta\mu^{aq}$ at a given temperature and pressure has been defined by Holder *et al.*⁴⁶ as:

$$\Delta\mu^{aq} / RT = \Delta\mu_o(T_o, p = 0 \text{ atm}) / RT_o - \int_{T_o}^T (\Delta H_w / RT^2) dT + (\Delta V_w / RT)p - \ln a_w \dots (2.7)$$

T and p are hydrate-formation temperature and pressure, T_o indicates the reference temperature, $273.15^\circ K$, R is the universal gas constant, and a_w is the water activity in the aqueous phase. The term of ΔV_w is molar volume associated with transition and ΔH_w (molar enthalpy difference) is independent of pressure and is defined by:

$$\Delta H_w = \Delta H_o + \int_{T_o}^T \Delta C_p dT \dots\dots\dots (2.8)$$

The term ΔC_p is a function of temperature and is given by:

$$\Delta C_p = a + b(T - T_o) \dots\dots\dots (2.9)$$

The values of the constants needed for calculation of $\Delta\mu^{aq}$ are given in **Table 2.4**.

Property	Unit	Structure I	Structure II
$\Delta\mu_o(liq)$	J/mol	1264	883
$\Delta H_o(liq)$	J/mol	-4858	-5201
$\Delta H_o(ice)$	J/mol	1151	808
$\Delta V_o(liq)$	Cm ³ /mol	4.6	5.0
$\Delta V_o(ice)$	Cm ³ /mol	3.0	3.4
$\Delta C_p(liq)$	J/mol/K	39.16	39.16

The chemical potential difference of water in the empty and the filled hydrate lattice was derived by van der Waals and Platteeuw⁴⁷ as follows:

$$\Delta\mu^H = RT \sum_i n_i \ln(1 - \sum_j f_j C_{ji}), \dots\dots\dots (2.10)$$

where n_i is the number of cavities of type i per water molecules, and f_j is fugacity of the component j in the gas phase and is determined by an equation of state, EOS. The parameter C_{ji} is the Langmuir adsorption constant, a function of temperature and specific for the cavity of type i and for component j .

$$C_{ji} = A/T \exp(B/T) \dots\dots\dots (2.11)$$

Constants A and B are unique for each component j that is capable of entering into a cavity of type i and must be determined from experimental data. These parameters are specific for the selected EOS and according to PVTsim,²⁰ for Structures I and II are mostly calculated by Munck *et al.*,²⁰ Rasmussen and Pederson,²⁰ and for Structure H by Madsen *et al.*²⁰

Table 2.5 and Table 2.6 give the values of the A and B parameters used in PVTsim.²⁰

TABLE 2.5—THE A AND B PARAMETERS FOR CALCULATING THE LANGMUIR CONSTANTS (SI & SII) ²⁰					
Gas	Structure	Small Cavity		Large Cavity	
		$A \times 10^3$ (K/atm)	B (K)	$A \times 10^3$ (K/atm)	B (K)
C ₁	I	0.7228	3187	23.35	2653
	II	0.2207	3453	100	1916
C ₂	I	0	0	3.039	3861
	II	0	0	240	2967
C ₃	II	0	0	5.455	4638
iC ₄	II	0	0	189.3	3800
nC ₄	II	0	0	30.51	3699
N ₂	I	1.671	2905	6.078	2431
	II	0.1742	3082	18	1728
CO ₂	I	0.00588	5410	3.36	3202
	II	0.0846	3602	846	2030
H ₂ S	I	10.06	2999	16.34	3737
	II	0.065	4613	252.3	2920
O ₂	I	17.4	2289	57.7	1935
	II	14.4	2383	154	1519
Ar	I	25.8	2227	75.4	1918
	II	21.9	2315	1866	1539

TABLE 2.6—THE A AND B PARAMETERS FOR CALCULATING THE LANGMUIR CONSTANTS (SH)²⁰				
Compound	Small Cavity		Large Cavity	
	$A \times 10^3$ (K/atm)	B (K)	$A \times 10^3$ (K/atm)	B (K)
C₁	2.800×10^{-4}	3390		
N₂	1.336×10^{-5}	3795		
iC₅			1.661×10^4	1699
Neohexane			1.627×10^3	3175
2,3-Dimethylbutane			1.747×10^2	3608
2,2,3-Trimethylbutane			8.066×10^8	-39
3,3-Dimethylpentane			2.826×10^3	3183
Methylcyclopentane			6.420×10^1	4024
1,2-Dimethylcyclohexane			3.912×10^1	5050
Cis-1,2-Dimethylcyclohexane			1.826×10^3	3604
Ethylcyclopentane			1.332×10^2	4207
Cyclooctane			1.647×10^3	4135

Replacing Eqs. 2.7 and 2.10 in Eq. 2.6 results in the following equation:

$$\Delta\mu_o(T_o, p = 0 \text{ atm}) / RT_o - \int_{T_o}^T (\Delta H_w / RT^2) dT + (\Delta V_w / RT) p - \sum_i n_i \ln(1 + \sum_j C_{ji} f_j) - \ln a_w = 0 \dots\dots\dots (2.12)$$

After calculating the water activity a_w from one of the equations derived by Javanmardi and Moshfeghian⁴ or Nasrifar and Moshfeghian,^{3, 8} Eq. 2.12 can be used to calculate the gas hydrate-formation temperature for a given pressure or gas hydrate pressure at a given temperature for a system containing aqueous electrolytes only or in the presence of both electrolytes and alcohol.

2.9 Equations of State (EOS)

An equation of state (EOS) relates the pressure (p), temperature (T), and volume (V) of a given system mathematically and is a tool that can predict the phase behavior and the volumetric properties of fluids. In hydrate prediction, an EOS can be used to determine the fugacity of each component in the gas phase (Eq. 2.10). Section 4.4 will discuss fugacity and its calculation using an EOS in more detail. Several EOS are available in the literature and each is useful for different applications. Cubic EOSes, the most commonly used in petroleum engineering, are cubic polynomials in volume. They are explicit in pressure and can be written as a sum of repulsion and attraction terms.

$$p = p_{\text{repulsion}} + p_{\text{attraction}} \dots\dots\dots (2.13)$$

The following equation has been defined by Soave-Redlich-Kwong (SRK)⁴⁸:

$$p = \frac{RT}{V-b} - \frac{a(T)}{V(V+b)} \dots\dots\dots (2.14)$$

where T, p, V , and R are the temperature, pressure, molar volume, and universal gas constant. The EOS parameters, a and b , have different values depending on the EOS; for a pure component, they are evaluated at the critical temperature using the following two equations:

$$\left(\frac{\partial p}{\partial V}\right)_{T_c} = 0 \dots\dots\dots (2.15)$$

$$\left(\frac{\partial^2 p}{\partial V^2}\right)_{T_c} = 0 \dots\dots\dots (2.16)$$

For component i , the parameter a at the critical point and parameter b are defined by:

$$a_{ci} = \Omega_a \frac{R^2 T_{ci}^2}{P_{ci}} \dots\dots\dots (2.17)$$

and

$$b_i = \Omega_b \frac{RT_{ci}}{P_{ci}} \dots\dots\dots (2.18)$$

with $\Omega_a = 0.42748$ and $\Omega_b = 0.08664$.

The parameter a is a function of temperature and can be defined as:

$$a_i(T) = a_{ci} \alpha_i(T) \dots\dots\dots (2.19)$$

$$\text{where } \alpha_i(T) = [1 + m(1 - \sqrt{T_r})]^2 \dots\dots\dots (2.20)$$

The term T_r is the reduced temperature (temperature divided by critical temperature) and m is given by:

$$m_i = 0.480 + 1.574\omega_i - 0.176\omega_i^2 \dots\dots\dots (2.21)$$

At the critical temperature, the right-hand side of the Eq. 2.20 is equal to 1 and consequently, in Eq. 2.19, $a_i(T)$ will be equal to a_{ci} . In Eq. 2.21 ω_i is the acentric factor and defined by Pitzer⁴⁹:

$$\omega_i = -\log p_{ri}^v(\text{at } T_{ri} = 0.7) - 1, \dots \quad (2.22)$$

p_{ri}^v is the reduced vapor pressure of component i (p / p_{ci}).

The parameters a and b for mixtures can be determined from the following mixing rules:

$$a_M = \sum_i \sum_j z_i z_j (a_i a_j)^{0.5} (1 - K_{ij}), \dots \quad (2.23)$$

and

$$b_M = \sum_i z_i b_i, \dots \quad (2.24)$$

where z_i and z_j represent the mole fractions of components i and j in the mixture and K_{ij} is the binary interaction coefficient between those components.

CHAPTER III

METHODOLOGY

3.1 Data Collection

In this research, I gathered over 1,400 data point at the three-phase equilibrium of different gas systems and used over 1,100 of them. The points that have not been considered in this development are mostly the points with high concentrations of inhibitors. For example, I removed those samples with electrolyte and methanol concentrations equal to or higher than 20 wt%, because adding inhibitors with higher concentrations is neither practical nor economic. I collected the data from Sloan² and literature published from 1940²⁻¹⁸ to 2004. My collection included data from pure components such as methane, carbon dioxide, ethane, propane, and hydrogen sulfide to natural gas systems in the presence of pure water, electrolytes and/or alcohols. A total of 12 hydrocarbons, three nonhydrocarbons, three electrolytes, and four thermodynamic inhibitors were involved in this development.

I used Marisoft Digitizer⁵⁰ software to translate data presented in graphic form only to tabulated data. To do this, I provided a JPEG file of those data reported in graphs, then by opening the file in Marisoft Digitizer environment and selecting the ranges for both X and Y axes, pointed on each experimental data point and transferred the digitized points to an Excel file. To have the temperature and pressure for all data in the same units, I converted all the different units of temperatures to °F and all the different units of pressures to psi, because these units are commonly used in the industry.

In this work, I used the Statistical Analysis Software (SAS)¹⁹ to find the best correlations among the variables, such as gas specific gravity and pseudoreduced pressure and temperature of gas mixtures, vapor pressure and liquid viscosity of water, and concentrations of electrolytes and thermodynamic inhibitors. Because of large number of independent variables, particularly hydrocarbons and nonhydrocarbons (15 components), I reduced those to only three variables, pseudoreduced temperature and pressure and gas

specific gravity, to represent all the gas components. The observations from the data gathered in this work show that in systems without inhibitors the gases with lower specific gravity form hydrates at higher pressure or lower temperature; these observations also show that the inclusion of some components such as propane, isobutene, and nitrogen causes different behavior for these systems. Taking into account all of these observations, I considered the use of specific gravity and pseudoreduced temperature and pressure as regression variables for developing these correlations.

The other regression variables, vapor pressure and liquid viscosity of water (especially water vapor pressure), were helpful in modeling the p -correlation, because the plot of vapor pressure of water versus temperature has the same shape as that for hydrate pressure versus temperature. Since the hydrate-formation process is considered to be a physical rather than a chemical process³⁶ (the guest molecules can rotate within the void spaces and no strong chemical bonds are formed between the hydrocarbon and water molecules), and because water is the most important element in this process, the physical properties of water such as liquid water viscosity at equilibrium could contribute to allowing the gas molecule to enter the void space as a guest.

The data include about 250 samples from pure components to binary, ternary and mixtures of gases in the presence of pure water, single and mixed inhibitors. The concentration ranges of each gas component and inhibitor along with the ranges of specific gravity, pressure, and temperature are summarized in **Table 3.1**.

TABLE 3.1—RANGE OF DIFFERENT INDEPENDENT VARIABLES FOR 1,104 DATA POINTS			
Variable	Mean	Minimum	Maximum
C₁	66.59	0	100
C₂	4.98	0	100
C₃	3.33	0	100
i-C₄	0.50	0	63.60
nC₄	0.38	0	5.82
i-C₅	0.004	0	0.20
nC₅	0.045	0	1.01
nC₆	0.005	0	0.25
nC₇	0.001	0	0.10
nC₈	0.0006	0	0.05
CO₂	18.66	0	100
N₂	3.45	0	89.20
H₂S	1.07	0	100
C₂H₄	0.92	0	94.40
C₃H₆	0.04	0	7.60
NaCl	1.98	0	17.17
KCl	0.53	0	15
CaCl₂	0.53	0	15.03
CH₃OH	1.81	0	19.99
Ethylene Glycol	0.69	0	30
Triethylene Glycol	0.16	0	20.20
Glycerol	0.43	0	30
Temperature, °F	46.33	10.29	89.33
Pressure, psi	1448.42	9.86	11240.42
Gas Specific Gravity ($\gamma_{air} = 1$)	0.829	0.5531	1.52

3.2 Data Observations

By screening the experimental data, I made some interesting observations. For example, for systems without inhibitors and at the same temperature, a system with lighter gas specific gravity usually forms hydrates at a higher pressure; this is consistent with the

results in the literature. However, that is not always the case and some of the data do not follow this pattern. By screening the experimental data and inspecting the compositions, I learned that some components have significant effects on the hydrate-formation pressure or temperature. For example, propane and isobutane will decrease the hydrate-formation pressure dramatically; however, nitrogen will increase it and act like an inhibitor.

Table 3.2 shows how the binaries of methane with propane, isobutane, or nitrogen decrease or increase the hydrate formation pressures at the same temperature for systems without inhibitors.

TABLE 3.2—EFFECTS OF GAS COMPOSITIONS ON HYDRATE-FORMATION PRESSURE IN SYSTEMS WITHOUT INHIBITORS				
Gas Compounds	Composition (mol%)	Hydrate Formation Temperature (°F)	Hydrate Formation Pressure (psi)	Gas Specific Gravity
C₁	100	39.11	552.59	0.5531
C₁ C₃	37.10 62.90	39.11	60.77	1.16172
C₁ N₂	27.20 72.80	39.11	1473.58	0.85359
C₁	100	39.29	565.65	0.5531
C₁ iC₄	71.4 28.6	39.29	51.63	0.9681
C₁ N₂	50.25 49.75	39.29	889.08	0.75845
C₁ N₂	10.80 89.20	39.29	2300.30	0.92128

This table shows that at 39.11°F, pure methane with specific gravity of 0.5531 forms hydrate at a pressure of 552.59 psi. At the same temperature for a binary of methane and nitrogen with higher specific gravity (0.85359), we expect hydrates to form at lower pressure, but the pressure is actually 1473.58 psi, which is higher than for the case of pure methane. This indicates that the hydrate-formation pressure does not always correlate negatively with specific gravity, and the presence of some components such as nitrogen in a mixture increases the hydrate-formation pressure.

Another example shows two binary systems of 97.50 mol% C₁ + 2.5 mol% i-C₄ and 97.50 mol% C₁ + 2.5 mol% nC₄, which both have the same gas specific gravity of 0.589, but the first binary will form hydrates at much lower pressures in a temperature range of 37.85 to 55.85°F. **Fig. 3.1** compares the hydrate-formation pressures for these systems. Although these two binary systems have the same molecular weight, they behave differently because the presence of some components such as isobutane in a mixture decreases the hydrate-formation pressure. Therefore, two systems with equal gas specific gravities do not necessarily form hydrates at equal pressures, but the presence of some components in a mixture has a very significant effect on determining the hydrate-formation pressure or temperature.

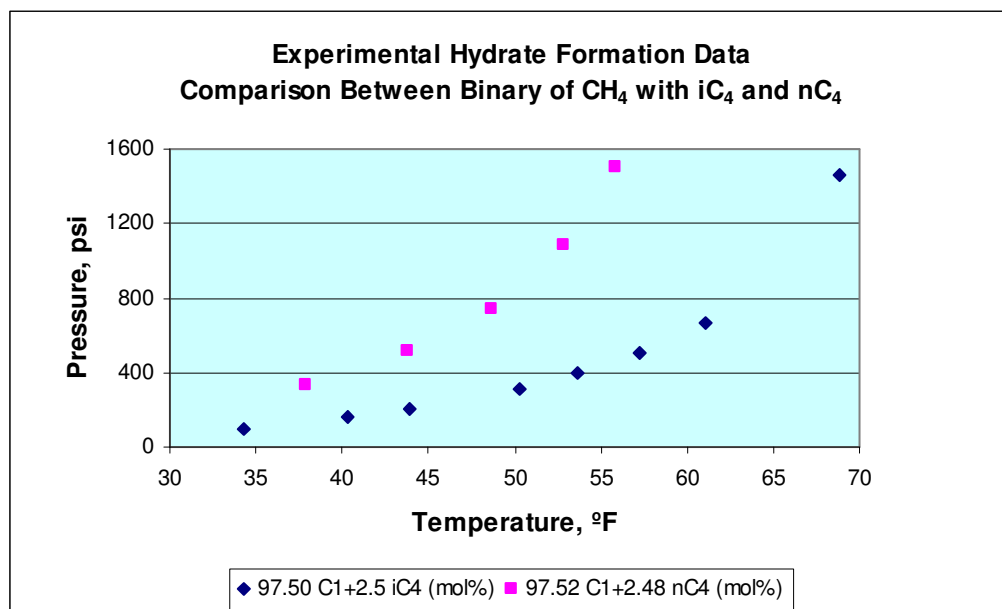


Fig. 3.1—Hydrate-formation pressure for binaries of CH₄ with iC₄ and nC₄.²

3.3 Comments on Data

1. Since Hammerschmidt discovered in 1934 that hydrates plug pipelines, a number of experiments have been done by different researchers; and less data have been measured in recent years than before. In addition, there are more data in the literature for the systems in the presence of pure water than with inhibitors.
2. I observed compositions in some data sets that did not total 100 mol%. People have used these data over and over to develop their predictive models or have reported them in their books and papers without noting that. For these types of data sets, I preferred to make up the deficiency of the compositions by adding to the methane mol% to normalize the compositions. I did that because in a natural gas methane usually has the highest fraction and adding one or two more mol% to methane does not affect the predicted results for hydrate-formation conditions.
3. Substantial existing data are the hydrate-formation conditions for gas systems that never or rarely exist in reality, such as pure hydrogen sulfide, pure propane, or pure ethane.
4. The experimental data reported in the literature, either graphically or digitized, have different units for temperature and pressure; to use these data I used digitizer software to translate those reported in graphs to tables and then to have the same units for all data I converted the different units to field units, °F for temperature and psi for pressure.

3.4 Regression Variables

The following equations show the calculation of the regression variables for developing the proposed correlations.

3.4.1 Pseudoreduced Temperature and Pressure

As we learned from the observation of experimental data, the gas compositions play an important role in determination of hydrate-formation pressure or temperature. By calculating the pseudoreduced temperature and pressure, we can take into account the effect of each component in the mixture. The pseudoreduced temperature and pressure

are defined as temperature or pressure of a system divided by pseudocritical temperature or pressure of the mixture of gas:

$$T_{pr} = T / T_{pc}, \dots \dots \dots (3.1)$$

and

$$p_{pr} = p / p_{pc}, \dots \dots \dots (3.2)$$

where T_{pr} and p_{pr} are the pseudoreduced temperature and pressure, and T_{pc} and p_{pc} are the pseudocritical temperature and pressure of gas mixtures.

To calculate T_{pc} and p_{pc} , I used the mixing rules of Piper *et al.*⁵¹ as follows:

$$T_{pc} = \frac{K^2}{J}, \dots \dots \dots (3.3)$$

and

$$p_{pc} = \frac{T_{pc}}{J}, \dots \dots \dots (3.4)$$

where J and K are defined by:

$$J = \alpha_0 + \sum_{i=1}^3 \alpha_i y_i \left(\frac{T_c}{P_c} \right) + \alpha_4 \sum_j y_j \left(\frac{T_c}{P_c} \right)_j, \dots \dots \dots (3.5)$$

and

$$K = \beta_0 + \sum_{i=1}^3 \beta_i y_i \left(\frac{T_c}{\sqrt{P_c}} \right) + \beta_4 \sum_j y_j \left(\frac{T_c}{\sqrt{P_c}} \right)_j, \dots \dots \dots (3.6)$$

where y_i is the mole fraction of nonhydrocarbon, y_j is the mole fraction of hydrocarbon components, $\alpha_0 - \alpha_4$ and $\beta_0 - \beta_4$ are constants as given in **Table 3.3**.

i	α_i	β_i
0	5.2073×10^{-2}	-3.9741×10^{-1}
1	1.0160×10^0	1.0503×10^0
2	8.6961×10^{-1}	9.6592×10^{-1}
3	7.2646×10^{-1}	7.8569×10^{-1}
4	8.5101×10^{-1}	9.8211×10^{-1}

The range of data for the mixing rules is summarized in **Table 3.4**.

Variable	Mean	Minimum	Maximum
H₂S	2.45	0.00	51.37
CO₂	3.38	0.00	67.16
N₂	1.87	0.00	15.68
C₁	71.15	19.37	94.73
C₂	8.21	2.30	18.40
C₃	4.04	0.06	12.74
iC₄	0.90	0.00	2.60
C₄	1.55	0.00	6.04
iC₅	0.64	0.00	2.24
C₅	0.88	0.00	3.92
C₆	0.65	0.00	4.78
Temperature, °F	243.8	78	326
Pressure, psia	3758.6	514	12814
Gas Specific Gravity ($\gamma_{air} = 1$)	0.972	0.613	1.821

3.4.2 Gas Specific Gravity

The specific gravity of the gas mixture is expressed as the molecular weight of the gas mixture divided by the molecular weight of air and is given by:

$$\gamma = \frac{\sum_i y_i MW_i}{MW_{air}}, \dots \dots \dots (3.7)$$

where MW_i and y_i are the molecular weight and mole fraction of component i in the mixture, and γ is the specific gravity of the mixture of gas.

3.4.3 Water Vapor Pressure

The vapor pressure measures the ability of molecules to escape from the surface of a solid or liquid. A common equation to estimate the vapor pressure of a component (in this case, water) is given by⁵²:

$$\log_{10}(p_w^v) = a_w^v + b_w^v / T + c_w^v \log_{10} T + d_w^v T + e_w^v T^2, \dots \dots \dots (3.8)$$

where T is the temperature of the system in °K, p_w^v is the vapor pressure of water in mmHg (must be converted to psi when used in Eq. 3.10) and a_w^v , b_w^v , c_w^v , d_w^v , and e_w^v are constants which for water at these units specified as follows:

$$a_w^v = 29.8605$$

$$b_w^v = -3.1522 \times 10^3$$

$$c_w^v = -7.3037$$

$$d_w^v = 2.4247 \times 10^{-9}$$

$$e_w^v = 1.8090 \times 10^{-6}$$

This equation is valid for the range of temperature from 273.16 to 647.13°K.

3.4.4 Liquid Water Viscosity

The viscosity measures the resistance of a substance to flow. Viscosity is affected by both temperature and pressure; for example, it decreases as temperature increases or pressure decreases. The following equation calculates the viscosity of liquid (in this case, water)⁵²:

$$\log_{10}(\mu_w^l) = a_w^l + b_w^l / T + c_w^l T + d_w^l T^2, \dots \quad (3.9)$$

where T is the temperature of the system in Kelvin, °K, μ_w^l is the viscosity of liquid water in centipoise, cp and a_w^l , b_w^l , c_w^l , and d_w^l are constants which for water at these units are as follows:

$$a_w^l = -10.2158$$

$$b_w^l = 1.7925 \times 10^3$$

$$c_w^l = 1.7730 \times 10^{-2}$$

$$d_w^l = -1.2631 \times 10^{-5}$$

This equation is valid for the range of temperature from 273 to 643°K.

3.5 Hydrate-Formation Pressure Correlation

I applied a regression model in SAS¹⁹ software to find the best relationships among the above mentioned regression variables. Eq. 3.10 is the result of this regression, the p -correlation, which predicts the hydrate-formation pressure at a given temperature:

$$\begin{aligned} \ln p_{pr} = & a_0 + a_1 \ln T_{pr} + a_2 \left[\left(\sum_i \frac{x_i}{M_i} \right) T_{pr} \right] / \gamma^2 + a_3 \left(\sum_i \frac{x_i}{M_i} \right) T_{pr} \\ & + a_4 \left[\left(\sum_j \frac{x_j}{M_j} \right) (x_{CO2} + x_{H2S} + x_{N2}) \left(\frac{1}{T_{pr}} \right)^2 + a_5 \left(\sum_j \frac{x_j}{M_j} \right) \left(\frac{1}{T_{pr}} \right) + a_6 [(\mu_w^l)^4 (T_{pr})^2 (p_w^v)] \right. \\ & + a_7 \left[(p_w^v) \left(\frac{1}{T_{pr}} \right) \right] + a_8 (T_{pr})^2 + a_9 \left[\left(100 - \sum_i x_i \right) (T_{pr})^2 \right] + a_{10} [(\ln \gamma)(T_{pr})] \\ & + a_{11} [(\ln \gamma)(\ln T_{pr})(p_w^v)] + a_{12} [(\ln \gamma)^2 (T_{pr})^2] + a_{13} [(\ln \gamma)(T_{pr})(p_w^v)^2] \\ & + a_{14} [(x_{C3} + x_{iC4})(T_{pr})^6] + a_{15} [(x_{C3} + x_{iC4})(p_w^v)(T_{pr})^6] + a_{16} [(x_{CO2} + x_{H2S})(\gamma) \left(\frac{1}{T_{pr}} \right)] \\ & + a_{17} [(x_{N2})(\gamma) \left(\frac{1}{T_{pr}} \right)^2] , \dots \quad (3.10) \end{aligned}$$

where T_{pr} and p_{pr} are the pseudoreduced temperature and pressure, γ is the specific gravity of the gas. The variable x_i indicates concentration of electrolytes such as sodium chloride (NaCl), potassium chloride (KCl), or calcium chloride (CaCl₂), and the variable x_j indicates concentration of thermodynamic inhibitors such as methanol, ethylene glycol, triethylene glycol, or glycerol, and both are expressed in weight percent. The variables p_w^v and μ_w^l are the water vapor pressure and liquid water viscosity, and a_0 to a_{17} are the coefficients of this correlation.

3.6 Hydrate-Formation Temperature Correlation

The following equation is the result of regression, the T -correlation, which predicts the hydrate-formation temperature when a pressure is given:

$$\begin{aligned} \ln T_{pr} = & b_0 + b_1(\ln p)^2 + b_2\left[\left(\sum_i \frac{x_i}{M_i}\right) / \gamma^2\right] + b_3\left[\left(\sum_j \frac{x_j}{M_j}\right) / \gamma^2\right] + b_4(\gamma^2) + b_5\left[(100 - \sum_i x_i)(\gamma^3)\right] \\ & + b_6(x_{CO_2} + x_{H_2S} + x_{N_2}) + b_7\left[\left(\sum_j \frac{x_j}{M_j}\right)(x_{CO_2} + x_{H_2S} + x_{N_2})\right] + b_8[(x_{C_3} + x_{iC_4}) / \gamma^6] \\ & + b_9[(\ln \gamma)(\ln p)] + b_{10}[(\ln \gamma)(\ln p)^4] + b_{11}[(\ln p) / \gamma] + b_{12}[(\ln p)^2 / \gamma] + b_{13}[(\ln p)^3 / \gamma] \\ & + b_{14}[(\ln p)^4 / \gamma] + b_{15}(\ln p_{pr}) + b_{16}(\ln p_{pr})^2, \dots \dots \dots (3.11) \end{aligned}$$

where constants b_0 to b_{16} are the coefficients of this correlation. The values of coefficients a_0 to a_{17} and b_0 to b_{16} are given in **Table 3.5**.

TABLE 3.5—VALUES OF CONSTANTS FOR HYDRATE-FORMATION p AND T CORRELATIONS				
i	a_i	Standard Error	b_i	Standard Error
0	-2.924729×10^0	8.031×10^{-2}	3.1113797464×10^0	2.319×10^{-2}
1	7.069408×10^0	3.424×10^{-1}	-6.121811×10^{-2}	5.4841×10^{-4}
2	-6.71674×10^{-1}	8.15×10^{-2}	$-3.4581592 \times 10^{-2}$	1.3×10^{-3}
3	2.158912×10^0	3.0819×10^{-1}	$-2.2257841 \times 10^{-2}$	1.06×10^{-3}
4	-1.4446×10^{-2}	1.6×10^{-3}	$-1.61387206 \times 10^{-1}$	9.5×10^{-3}
5	3.367516×10^0	9.032×10^{-2}	4.644864×10^{-4}	3.249×10^{-5}
6	-1.68816×10^{-1}	3.947×10^{-2}	6.0870675×10^{-3}	2.101×10^{-5}
7	1.3213962×10^1	3.0521×10^{-1}	-4.9726×10^{-4}	4.62×10^{-5}
8	2.365031×10^0	3.4994×10^{-1}	1.682281×10^{-4}	1.282×10^{-5}
9	-2.5796×10^{-2}	3.41×10^{-3}	$-1.93610096 \times 10^{-1}$	5.68×10^{-3}
10	2.461102×10^0	2.3531×10^{-1}	1.963793×10^{-4}	8.61×10^{-6}
11	-7.100059×10^0	1.50553×10^0	$1.324677497 \times 10^{-1}$	1.1×10^{-2}
12	1.820312×10^0	1.6222×10^{-1}	$-7.8512137 \times 10^{-2}$	4.03×10^{-3}
13	7.517561×10^0	6.8072×10^{-1}	9.232805×10^{-3}	4.9397×10^{-4}
14	-1.8793×10^{-2}	9.1908×10^{-4}	-2.32276×10^{-4}	2.148×10^{-5}
15	1.9029×10^{-2}	2.78×10^{-3}	$8.054836679 \times 10^{-1}$	3.98×10^{-3}
16	-5.307×10^{-3}	8.8911×10^{-4}	6.3403148×10^{-3}	1.04×10^{-3}
17	-3.2564×10^{-2}	5.44×10^{-3}		

CHAPTER IV

RESULTS AND DISCUSSION

Using the statistical analysis software (SAS),¹⁹ I applied a regression model for 1,104 experimental data points to find the best correlations among the variables. The data points include different samples from pure hydrocarbon and nonhydrocarbon components to gas mixtures. As can be seen from **Table 3.1**, besides temperature and pressure, 15 gas components, 3 electrolytes, and 4 thermodynamic inhibitors have entered the regression as independent variables. Section 3.3 included the calculations of the variables included in this regression. To check the accuracy of the correlations and compare the predicted results with the experimental data, I applied a statistical error analysis for both correlations.

4.1 Predicted Results Versus Experimental

Figs. 4.1 and **4.2** show the calculated results versus experimental for 1,104 data points. Using the following equation, the average absolute percentage error on pressure (p_{aae}) measures the statistical error for the p -correlation of 15.93 with the R^2 equal of 0.968:

$$p_{\text{aae}} = \left(\frac{100}{n} \right) \sum_i^n |p(\text{cal.})_i - p(\text{exp.})_i| / p(\text{exp.}), \dots \dots \dots (4.1)$$

The average of absolute temperature difference (T_{aad}) measures the statistical error from the following equation for the T -correlation of 2.97°F with the R^2 equal of 0.999:

$$T_{\text{aad}} = \sum_i^n |T(\text{cal.})_i - T(\text{exp.})_i| / n, \dots \dots \dots (4.2)$$

where n is the total number of the data points that have been used in developing the two correlations.

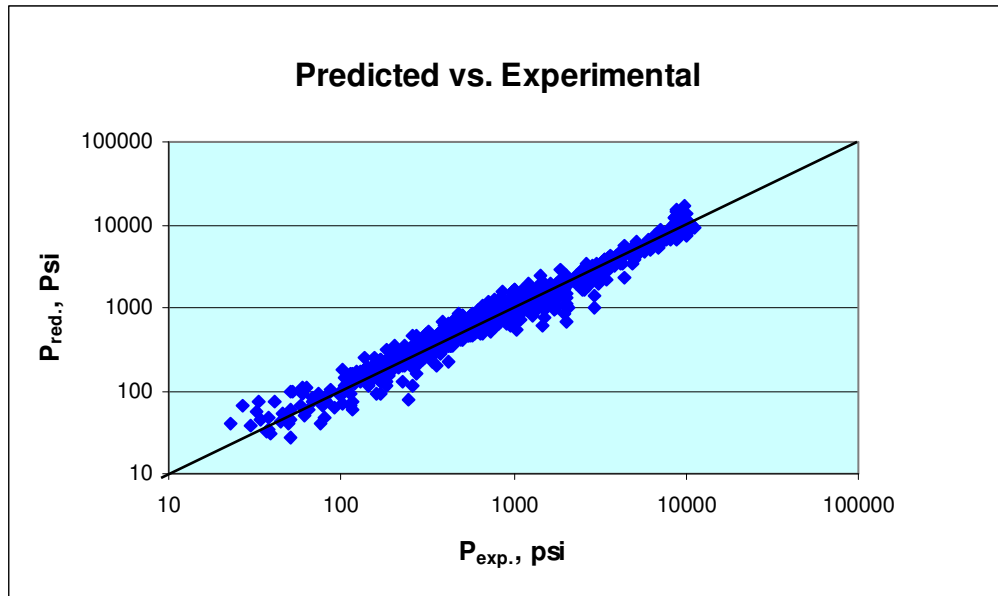


Fig. 4.1—Comparison of experimental and calculated values of hydrate-formation pressure (number of data points: 1,104, $R^2 = 0.968$, $p_{aae} = 15.93$).

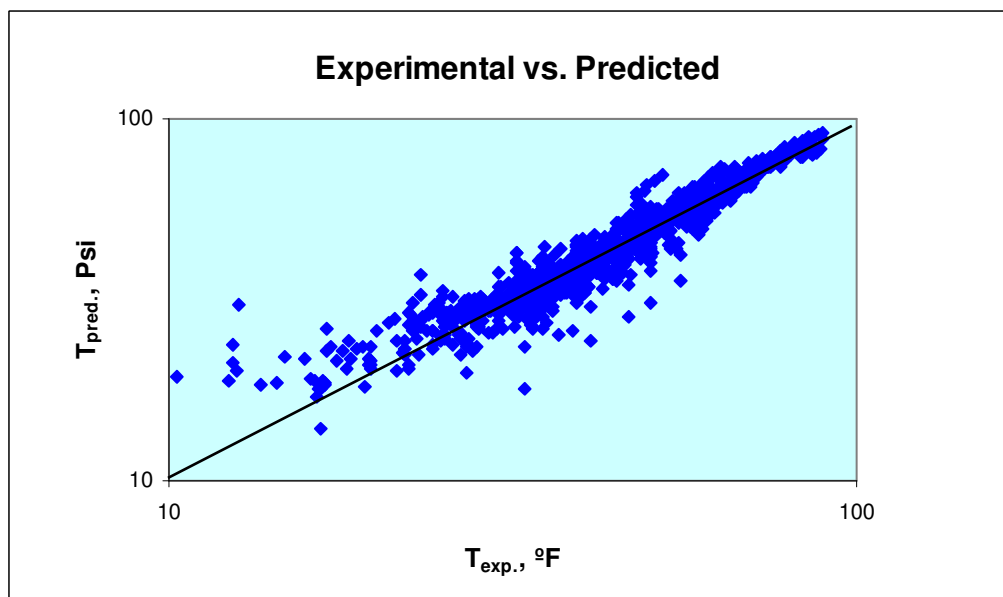


Fig. 4.2—Comparison of experimental and calculated values of hydrate-formation temperature (number of data points: 1,104, $R^2 = 0.999$, $T_{aad} = 2.97$).

Figs. 4.3 through 4.5 show the calculated hydrate-formation pressure from pressure correlation versus the experimental. Methane has been chosen for this comparison since it is a key component of any natural gas mixtures, and hydrates of methane are the most commonly found hydrates. **Fig. 4.3** shows an excellent agreement between the calculated hydrate-formation pressure and experimental data except a little deviation for the system of gas and electrolytes, which occurs only at high pressures. **Figs. 4.4 and 4.5** compare the calculated and experimental hydrate-formation pressure for two natural gas mixtures with the same components. In Fig. 4.4 where the gas mixture contains small concentrations of propane and nitrogen, the predicted results represent the experimental perfectly; however, Fig 4.5 shows slight deviation for predicted results from experimental data when the mixture contains higher fractions of these two components.

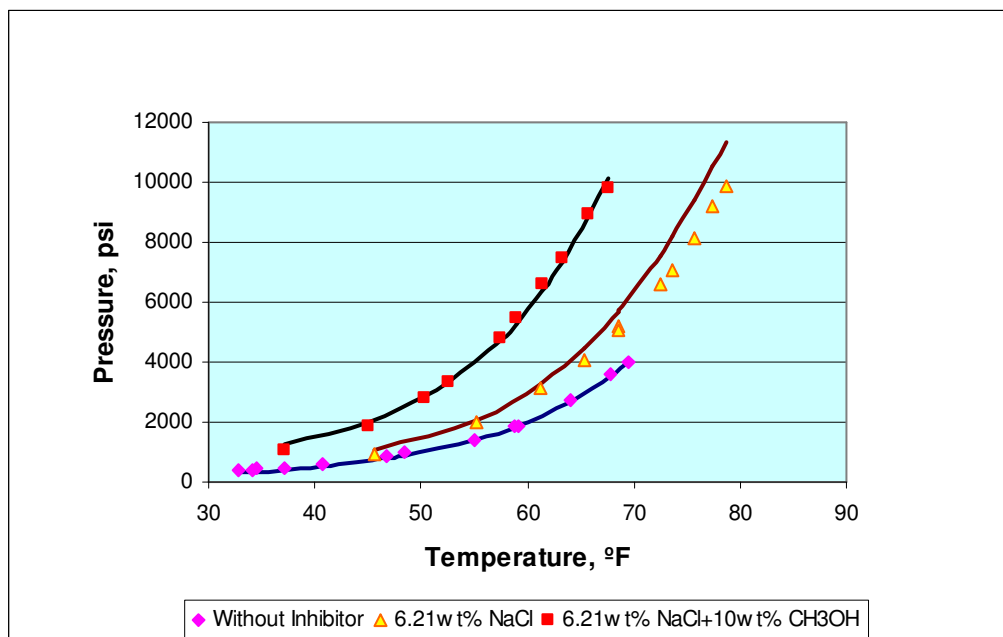


Fig. 4.3—Comparison of experimental and calculated results of hydrate-formation pressure from p -correlation for pure methane.

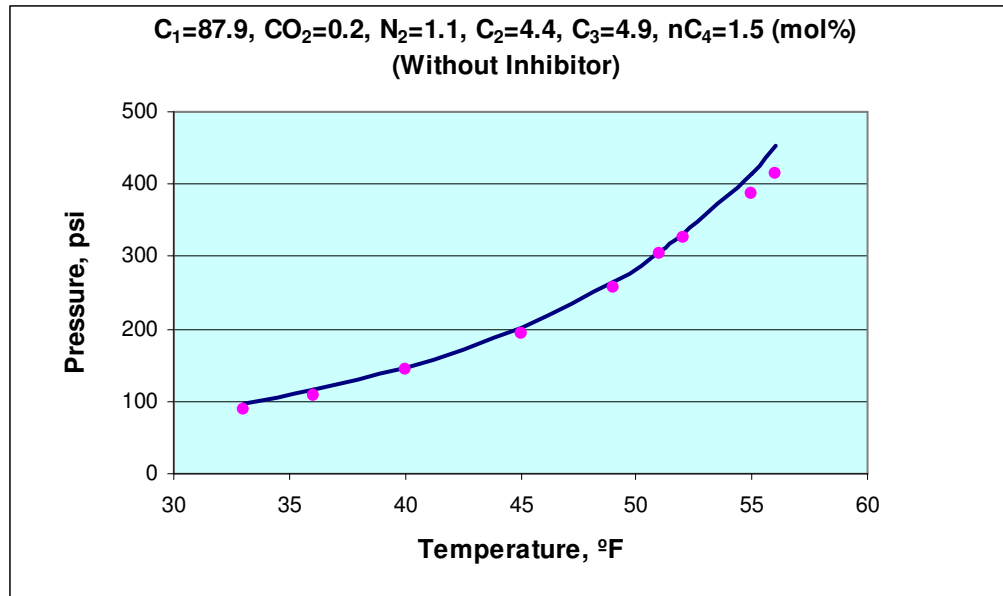


Fig. 4.4—Comparison of experimental and calculated results of hydrate-formation pressure from p -correlation for a natural gas with low concentration of propane and nitrogen.

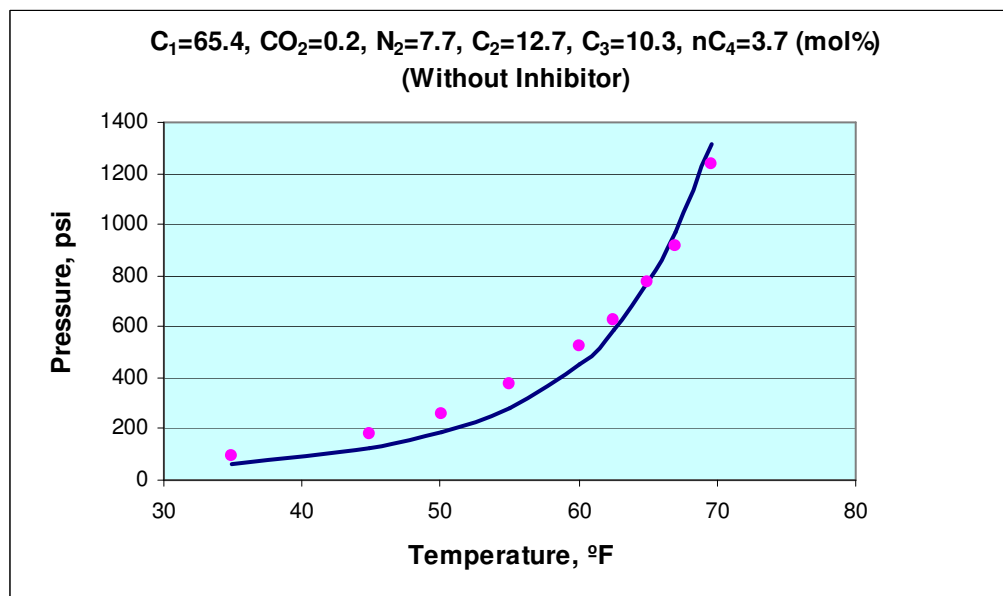


Fig. 4.5—Comparison of experimental and calculated results of hydrate-formation pressure from p -correlation for a natural gas with high concentration of propane and nitrogen.

Figs. 4.6 through 4.8 show the calculated hydrate-formation temperature from temperature correlation versus the experimental. **Fig. 4.6** shows the calculated results are in excellent agreement with experimental data except slight deviation at low temperatures for the complex system of gas and mixed inhibitors.

Figs. 4.7 and 4.8 compare the calculated and experimental hydrate-formation temperature for the same natural gas systems. In Fig. 4.7 where the gas mixture contains small concentrations of propane and nitrogen, the predicted results represent the experimental perfectly; however, Fig 4.8 shows deviation for predicted results from experimental when the mixture contains higher fractions of these two components. Despite of the deviation for this case, the calculated values still follow the same trend as the experimental.

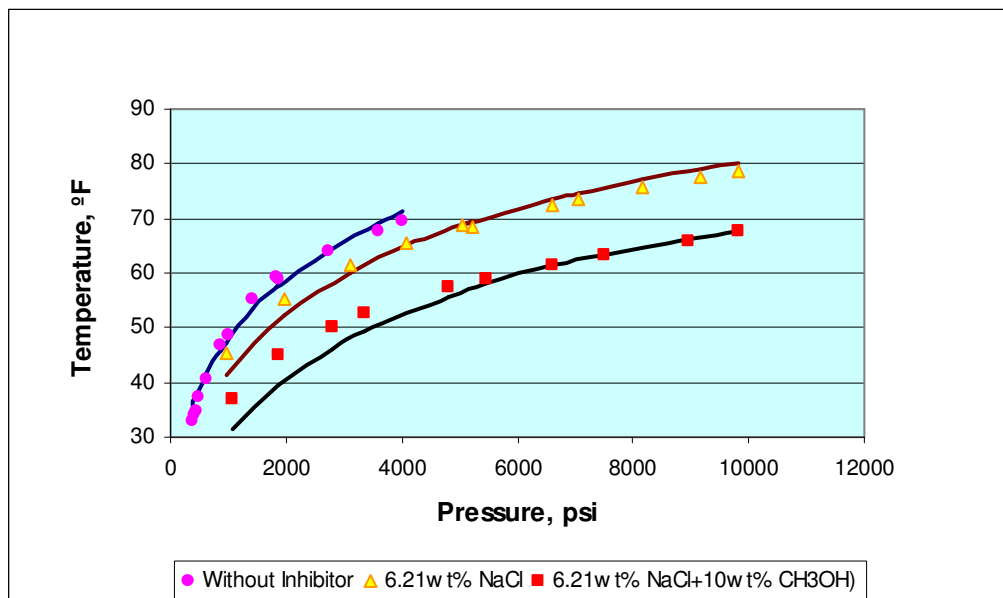


Fig. 4.6—Comparison of experimental and calculated results of hydrate-formation temperature from T -correlation for pure methane.

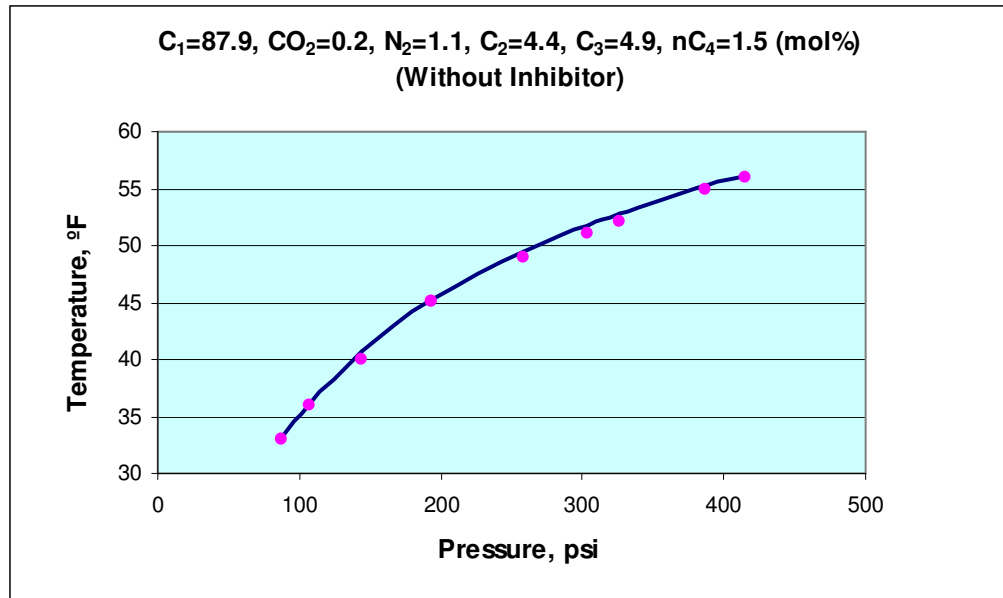


Fig. 4.7—Comparison of experimental and calculated results of hydrate-formation temperature from T -correlation for a natural gas with low concentration of propane and nitrogen.

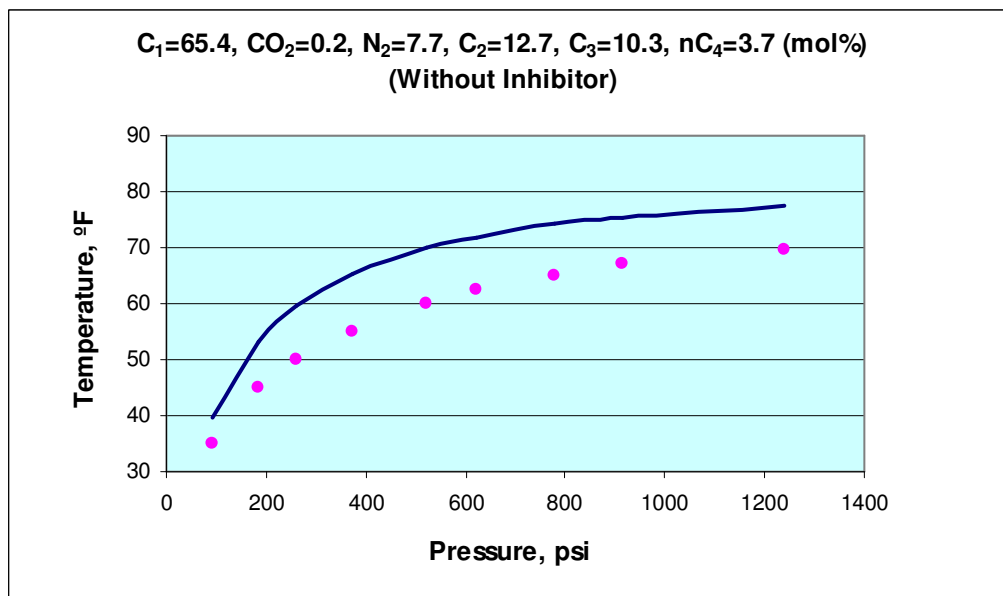


Fig. 4.8—Comparison of experimental and calculated results of hydrate-formation temperature from T -correlation for a natural gas with high concentration of propane and nitrogen.

4.2 Comparison of Predicted Results with a Common Correlation

As I mentioned earlier in Section 2.7.3, Kobayashi *et al.*⁴³ developed Eq. 2.3 from the gas-gravity plot from Katz. To compare the accuracy of the T -correlation with that of Kobayashi *et al.* equation, considering all the limitations for this equation (data included only hydrocarbons; data without inhibitors; data at pressures lower than 1,500 psia, specific gravities lower than 0.9, and temperatures between 0.34 and 62°F), I calculated the hydrate-formation temperature from both methods. For 173 data points from my collection, the results showed that my equation is superior to the Kobayashi *et al.* equation with an average absolute temperature difference of 2.87°F versus 13.02°F. **Fig. 4.9** shows the actual difference between predicted and experimental temperatures for my T -correlation and the Kobayashi *et al.* correlation.

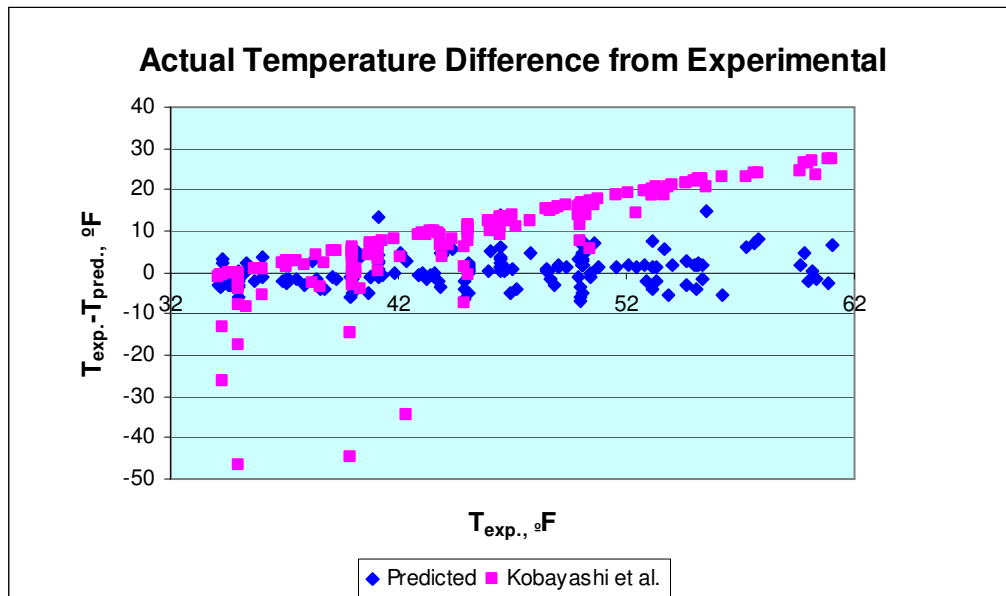


Fig. 4.9—Actual differences between predicted and experimental temperatures for T -correlation and Kobayashi *et al.* correlation.

4.3 Comparison of Predicted Results with Calculated from PVTsim

The results of the two improved correlations make them competitive even with the commercial software. To prove this claim, I have compared the results of the improved

correlations with the results from the available commercial software, PVTsim²⁰. For most sets of data, the results from the new correlations are as good as the results from PVTsim; however, for some of the data sets, these correlations predict the hydrate-formation conditions even better than PVTsim. **Figs. 4.10 and 4.11** compare the predicted hydrate-formation pressure and temperature from the correlations and PVTsim for two different natural gas systems.

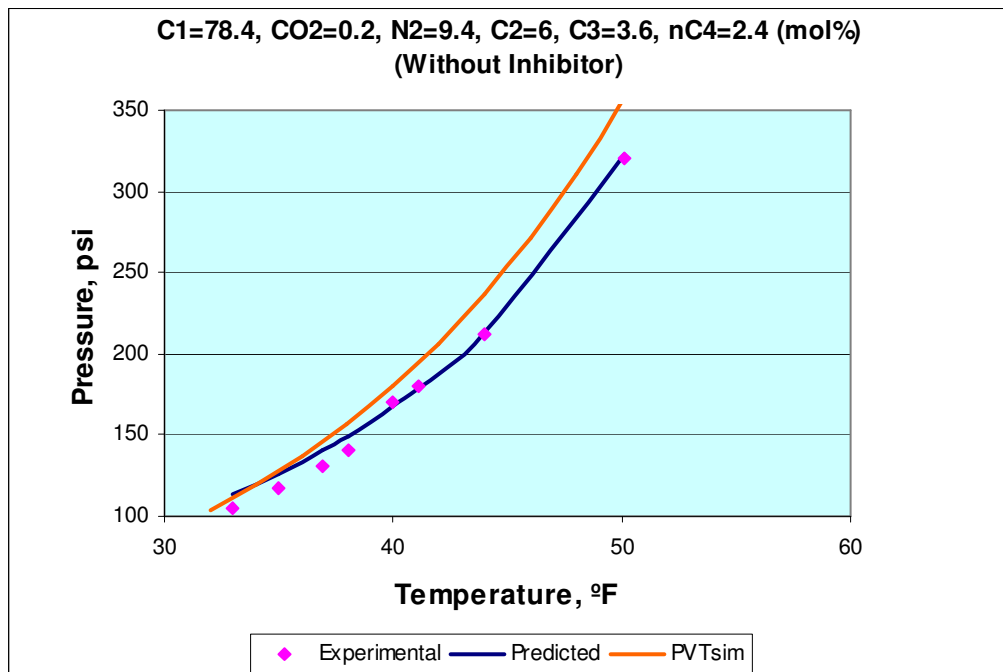


Fig. 4.10—Comparison of the calculated hydrate-formation pressure from PVTsim and *p*-correlation.

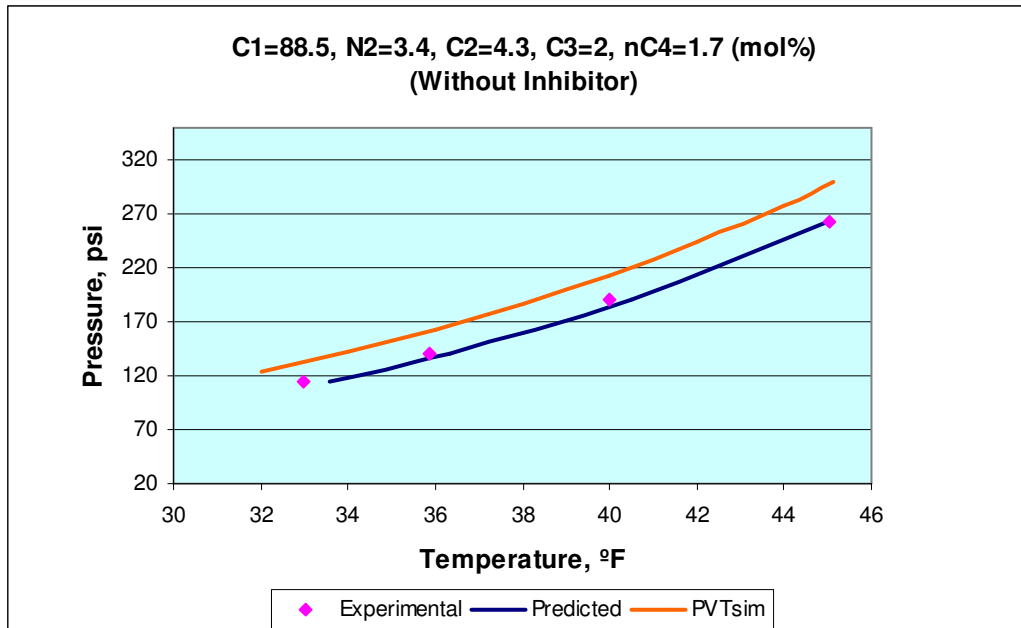


Fig. 4.11—Comparison of the calculated hydrate-formation temperature from PVTsim and T -correlation.

4.4 Sensitivity Analysis

The best way to determine the hydrate formation conditions is to measure the pressure and temperature experimentally. Since this is expensive and time consuming, the available correlations or thermodynamics methods can predict these conditions. When using a thermodynamics model, if the predicted results have significant deviations from the experimental data, it is possible to improve the model by adjusting the parameters entering into the model. Recall that one of the objectives of this work is to provide guidelines to calibrate a thermodynamics model by applying a sensitivity analysis to selective parameters entering into the model. To conduct the sensitivity analysis, we determined two possible parameters, binary interaction coefficients (K_{ij}) and the Langmuir adsorption constant (C_{ji}) in a thermodynamics model so that adjusting those parameters will cause the model to behave differently.

To predict the hydrate-formation conditions from a thermodynamics model, the chemical potential difference of water in the empty and in the filled hydrate lattice ($\Delta\mu^H$) requires calculation of fugacity for each component in the gas phase (Eq. 2.10). The fugacity of component i (f_i) is defined by:

$$f_i = \phi_i y_i p, \dots\dots\dots (4.3)$$

where ϕ_i = fugacity coefficient, y_i = mole fraction of component i in the gas phase, and p = pressure of the system. The fugacity coefficients ϕ_i can be determined from an EOS. For a given component the difference of its fugacity in one phase with respect to another phase is a value that measures the transfer potential of that component between the phases. Therefore, at equilibrium conditions when the fugacity of a component in the two or more phases is equal, there is no mass transformation across the phases; pressure, temperature, and the compositions within the phases remain constant.

The following equation is a thermodynamic relationship that determines the fugacity coefficient of component i in the mixture:

$$\ln \phi_i = -1/RT \int_{\infty}^V \left(\left(\frac{\partial p}{\partial n_i} \right)_{T,V,n_j} - \frac{RT}{V} \right) dV - \ln Z, \dots\dots\dots (4.4)$$

where n_i is the number of moles of type i .

In case of the SRK-equation²⁹:

$$\ln \phi_i = \left(\frac{b_i}{b} \right) (Z - 1) - \ln Z + \ln \left[\frac{V}{(V - b)} \right] + \frac{a}{bRT} \left[\frac{b_i}{b} - 2 \sum_j \frac{Z_j (1 - K_{ij}) (a_i a_j)^{0.5}}{a} \right] \ln \left[\frac{(V + b)}{V} \right] \dots\dots\dots (4.5)$$

PVTsim²⁰ has different options to calculate the binary interaction coefficient K_{ij} ; however, this software supports the following temperature-dependent binary interaction K_{ij} :

$$K_{ij} = K_{ij}A + cn_j [K_{ij}B + K_{ij}C(T - T_0)], \dots \dots \dots (4.6)$$

where $K_{ij}A$, $K_{ij}B$, and $K_{ij}C$ are user input; T_0 is a reference temperature of 288.15°K; and cn_j is the carbon number of component j . The attempt to adjust the variables $K_{ij}A$, $K_{ij}B$, and $K_{ij}C$ failed because the software does not accept the changes.

PVTsim considers three types of hydrate lattices, SI, SII and SH. Hydrates with structures I and II consist of two different sizes of cavities, small and large. Structure H consists of three different sizes of cavities which in PVTsim are modeled as two cavity sizes, small/medium and huge. As we saw in Section 2.8, the Langmuir adsorption constant C_{ji} is a temperature-dependent parameter and the values of A and B (Eq. 2.11) are unique for each component j that is capable of entering into a cavity of type i . For example, the value of A for component C_1 that enters a large cavity of SII is equal to 1.335×10^{-1} °F/psia, and with this value we saw the prediction from PVTsim in **Fig. 4.10** that deviated from experimental. Multiplying the value of A by 10, PVTsim shows better results, as can be seen in **Fig. 4.12**. Similarly, the value of A for component C_2 that enters a large cavity of SI is equal to 3.722×10^{-4} °F/psia, and by making this value 10 times larger, PVTsim shows better results, as we see in **Fig. 4.13**.

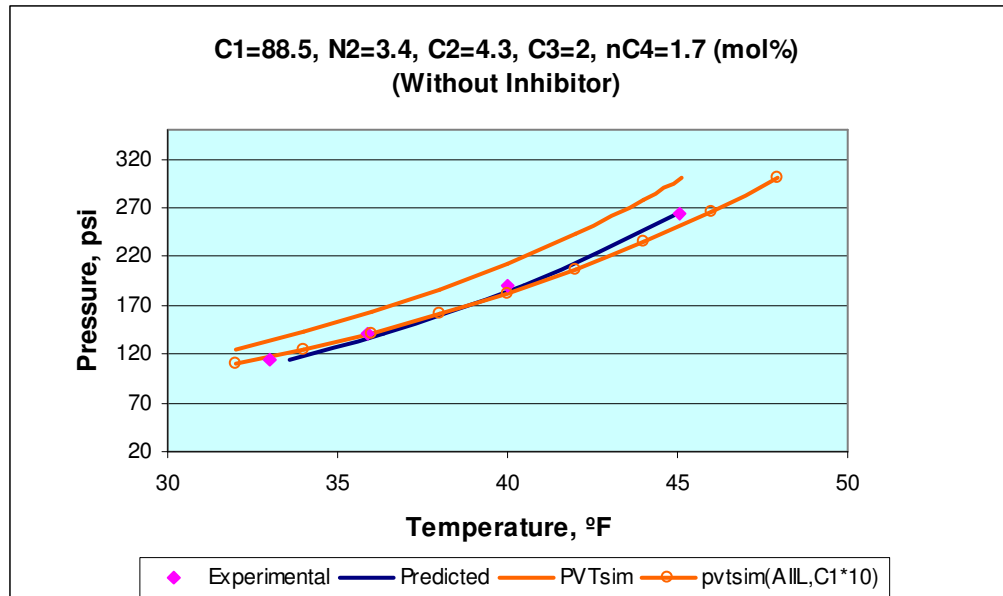


Fig. 4.12—Calculated results from PVTsim before and after adjusting the value of A for component C_1 in a large cavity of Structure II.

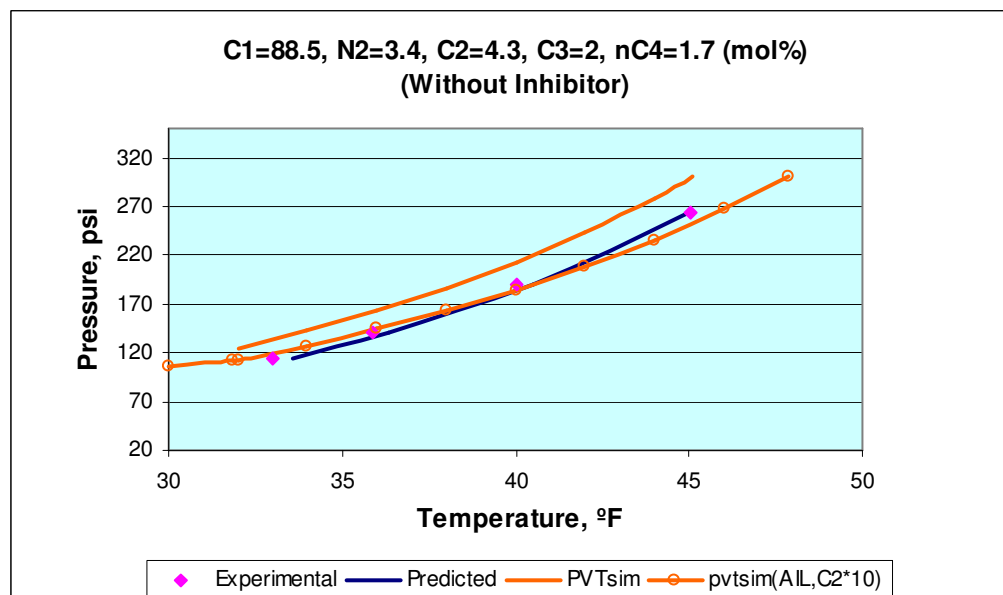


Fig. 4.13—Calculated results from PVTsim before and after adjusting the value of A for component C_2 in a large cavity of Structure I.

Therefore, the predicted results from PVTsim are sensitive to the A parameter for some components in large cavities of SI and SII. Although the hydrate types and the sizes of cavities do not affect our correlation, from the sensitivity analysis for PVTsim, we can reach the conclusion that our correlations could be sensitive to some or all of the variables involved in their development. This means that we can probably improve the new correlations by adjusting the current variables, by entering new variables such as density of water, or even by using improved mixing rules with a wider range of hydrocarbon, temperatures, and pressures. The mixing rule that I used to calculate the pseudoreduced temperature and pressure is limited to some ranges of composition, temperature, and pressure which do not cover all the ranges for the experimental data; that could affect the accuracy of the new correlations to some extent. By having more experimental data and considering other regression variables, it is possible to improve these correlations more and more.

CHAPTER V

CONCLUSIONS

Gas hydrates are a costly problem when they plug oil and gas pipelines. The best way to determine the hydrate-formation temperature and pressure is to measure these conditions experimentally for every gas system. Since this is not practical in terms of time and money, correlations are the other alternative tool. Only a couple of the thermodynamics methods in the literature are applicable for systems including inhibitors. In this work, we introduced two improved correlations that calculate the hydrate-formation pressure or temperature for single gases or mixtures of gases with or without inhibitors. These correlations are based on over 1,100 published data points of gas-hydrate formation temperatures and pressures with and without inhibitors. The data include samples ranging from pure-hydrate formers such as methane, ethane, propane, carbon dioxide, and hydrogen sulfide to binary, ternary, and natural gases. Using the Statistical Analysis Software (SAS),¹⁹ we found the best correlations among the variables including gas specific gravity, pseudoreduced pressure and temperature of gas mixtures, vapor pressure and liquid viscosity of water, and concentrations of electrolytes and thermodynamic inhibitors.

These correlations are applicable to temperatures up to 90°F and pressures up to 12,000 psi and they are capable of handling aqueous solutions containing electrolytes such as sodium, potassium, and calcium chlorides lower than 20 wt% and inhibitors such as methanol lower than 20 wt%, ethylene glycol, triethylene glycol, and glycerol lower than 40 wt%. The results show an average absolute percentage deviation of 15.93 in pressure and an average absolute temperature difference of 2.97°F.

The improved correlations are simple and portable since they are applicable even with a simple calculator. The results are in excellent agreement with the experimental data in most cases and even better than the results from commercial simulators in some cases. These correlations provide guidelines to help the users to forecast gas-hydrate forming conditions for most systems of hydrate formers with and without inhibitors.

My conclusions of this research come in two parts, conclusions from my observations of experimental data which are consistent with what I read in the literature and conclusions from my work in developing the improved correlations.

5.1 Conclusions from Observations

- In absence of inhibitors and at the same temperature, a gas with lighter specific gravity forms hydrates at higher pressure, but we should consider the presence of components such as propane, isobutane, and nitrogen. The presence of propane and isobutane in a gas mixture decreases the hydrate-formation pressure and increases the hydrate-formation temperature, while the presence of nitrogen in a gas mixture increases the hydrate-formation pressure and decreases the hydrate-formation temperature.
- Compositions of a gas system play a very important role in determining the hydrate-formation temperature or pressure. That means two gas systems with equal specific gravity may form hydrates at very different conditions. For instance, a binary mixture of methane and isobutane forms hydrates at lower pressure and higher temperature than a mixture of methane and butane with the same composition and specific gravity.
- Sodium chloride has a higher inhibition effect than methanol at the same concentration; this is very obvious at higher pressures. In the presence of mixed inhibitors, the inhibitor with higher concentration of sodium chloride is more effective than the one with higher concentration of methanol.
- The inhibition effect of ethylene glycol is inferior to that of methanol at the same concentration.

5.2 Conclusions from Developing the Improved Correlations

- The improved correlations estimate the hydrate-formation temperature or pressure for a variety of gas-hydrate formers in the presence or absence of inhibitors.
- These correlations are easy to use and they are applicable even with a simple calculator.

- The predicted results are in a good agreement with the experimental data in most cases.
- These correlations are very accurate and in some cases they can predict the hydrate-formation conditions even better than the commercial software, PVTsim.
- The improved correlations are unique since none of the available correlations in the literature can predict the hydrate-formation conditions for complex systems including inhibitors; in addition, the new correlations proved to be much more accurate than the common correlations.
- The results from 1,104 data points show an average absolute percentage deviation of 15.93 in pressure for the p -correlation and an average absolute temperature difference of 2.97°F for the T -correlation.
- The correlations are useful for a wide range of temperature (to 90°F) and pressure (to 12,000 psi).
- A sensitivity analysis on parameter A of the Langmuir adsorption constant showed that the value of this parameter for hydrocarbons entering in large cavities of Structures I and II has significant effect on the calculated hydrate-formation temperature and pressure by PVTsim simulator.

NOMENCLATURE

a_w	=	water activity
$a.a.T.d.$	=	average of absolute temperature difference
$a.a.p.e.$	=	average of absolute percentage error on pressure
C_{ji}	=	Langmuir adsorption constant
C_p	=	molar heat capacity
f_i	=	fugacity of gas component in a gas mixture
H	=	molar enthalpy
k_{ij}	=	binary interaction coefficient
K^{vs}	=	vapor/solid equilibrium ratio
M_{air}	=	molecular weight of air
M_i	=	molecular weight of electrolyte i
M_j	=	molecular weight of thermodynamic inhibitor j
MW_i	=	molecular weight of component i in a gas mixture
n	=	number of data points
n_i	=	number of cavities of type i per water molecules
p	=	pressure of the system
p_c	=	critical pressure
p_{pc}	=	pseudocritical pressure
p_{pr}	=	pseudoreduced pressure
p_r^v	=	reduced vapor pressure
p_w^v	=	vapor pressure of water
R	=	universal gas constant
s_i	=	mol fraction of component i in solid phase
T	=	temperature of the system
T_c	=	critical temperature

T_{pc}	=	pseudocritical temperature
T_{pr}	=	pseudoreduced temperature
T_r	=	reduced temperature
T_0	=	reference temperature
V	=	molar volume
y_i	=	mol fraction of component i in vapor phase
x_i	=	concentration of electrolyte i
x_j	=	concentration of thermodynamic inhibitor j
Δ	=	difference in properties
ϕ	=	fugacity coefficient
γ	=	gas specific gravity
μ	=	chemical potential
μ_w^l	=	viscosity of liquid water
ω	=	acentric factor

REFERENCES

1. Hammerschmidt, E.G.: "Formation of Gas Hydrates in Natural Gas Transmission Lines," *Industrial & Engineering Chemistry* (1934) **26**, 851.
2. Sloan, E.D. Jr.: *Clathrate Hydrates of Natural Gases*, Marcel Dekker, New York (1990).
3. Nasrifar, K. and Moshfeghian, M.: "A Model for Prediction of Gas Hydrate Formation Conditions in Aqueous Solutions Containing Electrolytes and/or Alcohol," *J. Chem. Thermodynamics* (2001) **33**, 999.
4. Javanmardi, J. and Moshfeghian, M.: "A New Approach for Prediction of Gas Hydrate Formation Conditions in Aqueous Electrolyte Solutions," *Fluid Phase Equilibria* (2000) **168**, 135.
5. Bishnoi, P.R. and Dholabhai, P.D.: "Equilibrium Conditions for Hydrate Formation for a Ternary Mixture of Methane, Propane and Carbon Dioxide, and a Natural Gas Mixture in the Presence of Electrolytes and Methanol," *Fluid Phase Equilibria* (1999) **158-160**, 821.
6. Dholabhai, P.D., Parent, J.S., and Bishnoi, P.R.: "Equilibrium Conditions for Hydrate Formation from Binary Mixture of Methane and Carbon Dioxide in the Presence of Electrolytes, Methanol and Ethylene Glycol," *Fluid Phase Equilibria* (1997) **141**, 235.
7. Nasrifar, K. and Moshfeghian, M.: "Computation of Equilibrium Hydrate Formation Temperature for CO₂ and Hydrocarbon Gases Containing CO₂ in the Presence of an Alcohol, Electrolytes and Their Mixtures," *J. of Petroleum Science and Engineering* (2000) **26**, 143.
8. Nasrifar, K., Moshfeghian, M., and Maddox, R.N.: "Prediction of Equilibrium Conditions for Gas Hydrate Formation in the Mixtures of Both Electrolytes and Alcohol," *Fluid Phase Equilibria* (1998) **146**, 1.
9. Dimitrios, A. and Varotsis, N.: "Modeling Gas Hydrate Thermodynamic Behavior: Theoretical Basis and Computational Methods," *Fluid Phase Equilibria* (1996) **123**, 107.

10. Du, Y. and Guo, T.: "Prediction of Hydrate Formation for Systems Containing Methanol," *Chemical Engineering Science* (1990) **45**, 893.
11. Ng, H.J. and Robinson, D.B.: "Hydrate Formation in Systems Containing Methane, Ethane, Propane, Carbon Dioxide or Hydrogen Sulfide in the Presence of Methanol," *Fluid Phase Equilibria* (1985) **21**, 145.
12. Jager, M.D., Peters, C.J., and Sloan, E.D.: "Experimental Determination of Methane Hydrate Stability in Methanol and Electrolyte Solutions," *Fluid Phase Equilibria* (2002) **193**, 17.
13. Jager, M.D. and Sloan, E.D.: "The Effect of Pressure on Methane Hydration in Pure Water and Sodium Chloride Solutions," *Fluid Phase Equilibria* (2001) **185**, 89.
14. Jossang, A. and Stange, E.: "A New Predictive Activity Model for Aqueous Salt Solutions," *Fluid Phase Equilibria* (2001) **181**, 33.
15. Ma, Q.L., Chen, G.J., and Guo, T.M.: "Modeling the Gas Hydrate Formation of Inhibitor Containing Systems," *Fluid Phase Equilibria* (2003) **205**, 291.
16. Ma, C.F., Chen, G.J., Wang, F., Sun, C.Y., and Guo, T.M.: "Hydrate Formation of (CH₄+C₂H₄) and (CH₄+C₃H₆) Gas Mixtures," *Fluid Phase Equilibria* (2001) **191**, 41.
17. Chen, G.J. and Guo, T.M.: "Thermodynamic Modeling of Hydrate Formation Based on New Concepts," *Fluid Phase Equilibria* (1996) **122**, 43.
18. Fan, S.S., Chen, G.J., Ma, Q.L., and Guo, T.M.: "Experimental and Modeling Studies on the Hydrate Formation of CO₂ and CO₂-Rich Gas Mixtures," *Chemical Engineering J.* (2000) **78**, 173.
19. SAS software, Version 8.02, SAS Institute Inc., Cary, North Carolina, (2001).
20. PVTsim software, Version 14, Calsep, Houston, Texas, (2004).
21. Tohidi, B., Danesh, A., Burgass, R.W., and Todd, A.C.: "Effect of Heavy Hydrate Formation on the Hydrate Free Zone of Real Reservoir Fluids," paper SPE 35568 presented at the 1996 European Production Operations Conference and Exhibition, Stavanger, Norway, 16-17 April.
22. von Stackelberg, M. and Muller, H.R.: "On the Structure of Gas Hydrates," *J. of Chemical Physics* (1951) **19**, 1319.

23. Claussen, W.F.: "Suggested Structures of Water in Inert Gas Hydrates," *J. of Chemical Physics* (1951) **19**, 259.
24. Claussen, W.F.: "A Second Water Structure for Inert Gas Hydrates," *J. of Chemical Physics* (1951) **19**, 1425.
25. Heriot Watt University, Institute of Petroleum Engineering, "What Are Gas Hydrates?" www.pet.hw.ac.uk/hydrate/hydrates_what_html, (2005).
26. McMullan, R.K. and Jeffrey, G.A.: "Hydrates of the Tetra n-Butyl and Tetra i-Amyl Quaternary Ammonium Salts," *J. of Chemical Physics* (1959) **31**, 1231.
27. McMullan, R.K. and Jeffrey, G.A.: "Polyhedral Clathrate Hydrates. IX. Structure of Ethylene Oxide Hydrate," *J. of Chemical Physics* (1965) **42**, 2725.
28. Mak, T.C.W. and McMullan, R.K.: "Polyhedral Clathrate Hydrates. X. Structure of the Double Hydrate of Tetrahydrofuran and Hydrogen Sulfide," *J. of Chemical Physics* (1965) **42**, 2732.
29. Pederson, K.S., Fredenslund, A.A, and Thomassen, P.: *Properties of Oils and Natural Gases*, Gulf Publishing Co., Houston, Texas, (1989).
30. Ripmeester, J.A., Tse, J.S., Ratcliffe, C.I., and Powell, B.M.: "A New Clathrate Hydrate Structure," *Nature* (1987) **325**, 135.
31. Tohidi, B., Danesh, A., Burgass, R.W., and Todd, A.C.: "Equilibrium Data and Thermodynamic Modeling of Cyclohexane Gas Hydrates," *Chemical Engineering Science* (1996) **51**, 159.
32. Tohidi, B., Danesh, A., Todd, A.C., Burgass, R.W., and Ostergaard, K.K.: "Equilibrium Data and Thermodynamic Modeling of Cyclopentane and Neopentane Hydrates," *Fluid Phase Equilibria* (1997) **138**, 241.
33. Becke, P., Kessel, D., and Rahimian, I.: "Influence of Liquid Hydrocarbons on Gas Hydrate Equilibrium," paper SPE 25032 presented at the 1992 European Petroleum Conference, Cannes, France, 16-18 November.
34. Ostergaard, K.K., Tohidi, B., Danesh, A., Burgass, R.W., and Todd, A.C.: "Equilibrium Data and Thermodynamic Modeling of Isopentane and 2, 2-Dimethylpentane Hydrates," *Fluid Phase Equilibria* (2000) **169**, 101.

35. Mehta, A.P. and Sloan, E.D.: "Structure H Hydrates: Implications for the Petroleum Industry," paper SPE 36742 presented at the 1996 Annual Technical Conference and Exhibition Denver, Colorado, 6-9 October.
36. McCain, W.D. Jr.: *The Properties of Petroleum Fluids*, PennWell Publishing Co., Tulsa, Oklahoma (1990).
37. Paez, J.E., Blok, R, Vaziri, H., and Islam, M.R.: "Problems in Gas Hydrates: Practical Guidelines for Field Remediation," paper SPE 69424 presented at the 2001 Latin American and Caribbean Petroleum Engineering Conference, Buenos Aires, Argentina, 25-28 March.
38. Ng, H.J., Petrunia, J.P., and Robinson, D.B.: "Experimental Measurement and Prediction of Hydrate Forming Conditions in Nitrogen-Propane-Water," *Fluid Phase Equilibria* (1977/1978) **1**, 283.
39. Ng, H.J and Robinson, D.B.: "The Measurement and Prediction of Hydrate Formation in Liquid Hydrocarbon-Water System," *Industrial & Engineering Chemistry Fundamentals* (1976) **15**, 293.
40. Bishnoi, P.R. and Dholabhai, P.D.: "Experimental Study on Propane Hydrate Equilibrium Conditions in Aqueous Electrolyte Solutions," *Fluid Phase Equilibria* (1993) **83**, 455.
41. Katz, D.L., Cornell, D., Kobayashi, R., Poettmann, F.H., Vary, J.A. *et al.*: "Water/Hydrocarbon Systems," *Handbook of Natural Gas Engineering*, McGraw-Hill, New York (1959).
42. Wilcox, W.I., Carson, D.B., and Katz, D.L.: "Natural Gas Hydrates," *Industrial & Engineering Chemistry* (1941) **33**, 662.
43. Kobayashi, R., Song, K.Y., and Sloan, E.D.: "Phase Behavior of Water/Hydrocarbon Systems," *Petroleum Engineering Handbook*, H.B. Bradley (ed.) SPE, Richardson, Dallas, Texas (1987).
44. Elgibaly, A.A. and Elkamel, A.M.: "A New Correlation for Predicting Hydrate Formation Conditions for Various Gas Mixtures and Inhibitors," *Fluid Phase Equilibria* (1998) **152**, 23.

45. Parrish, W.R. and Prausnitz, J.M.: "Dissociation Pressures of Gas Hydrates Formed by Gas Mixtures," *Industrial & Engineering Chemistry Process Design and Development* (1972) **11**, 26.
46. Holder, G.D., Zetts, S.P., and Pradhan, N.: "Phase Behavior in Systems Containing Clathrate Hydrates," *Review in Chemical Engineering* (1988) **5**, 1.
47. van der Waals, J.H. and Platteeuw, J.C.: "Clathrate Solutions," *Adv. Chem. Phys.* (1952) **2**, 1.
48. Soave, G.: "Equilibrium Constants from a Modified Redlich-Kwong Equation of State," *Chemical Engineering Science* (1972) **27**, 1197.
49. Pitzer, K.S.: "The Volumetric and Thermodynamic Properties of Fluids. I. Theoretical Basis and Virial Coefficients," *J. of the American Chemical Society* (1955) **77**, 3427.
50. Marisoft Digitizer, Version 3.3, Mark Mitchell, (1997). [Available at <http://home.earthlink.net/~mmc1919>].
51. Piper, L.D., McCain, W.D., and Corredor, J.H.: "Compressibility Factors for Naturally Occurring Petroleum Gases," paper SPE 69424 presented at the 1993 Annual Technical Conference and Exhibition, Houston, 3-6 October.
52. Yaws, C.L.: *Chemical Properties Handbook*, McGraw-Hill, New York (1999).

APPENDIX A
EXPERIMENTAL DATA

The entire experimental data gathered and used in this work is in a separate Excel file.

APPENDIX B

HYDRATE-FORMATION PRESSURE CALCULATION

This Excel file includes a Visual Basic program that calculates the hydrate-formation pressure at a given temperature. By giving the gas composition and the inhibitor concentration as input data to this program, a user can calculate the hydrate-formation pressure at a given temperature for that system. This calculation can be done very quick and only by clicking on the Hydrate Pressure button in the Data sheet.

APPENDIX C

HYDRATE-FORMATION TEMPERATURE CALCULATION

This Excel file includes a Visual Basic program that calculates the hydrate-formation temperature at a given pressure. By giving the gas composition and the inhibitor concentration as input data to this program, a user can calculate the hydrate-formation temperature at a given pressure for that system. This calculation can be done very quick and only by clicking on the Hydrate Temperature button in the Data sheet.

VITA

Name: Sharareh Ameripour

Permanent Address: 22015 Velicata
Woodland Hills, CA 91364

Education: M.S., Petroleum Engineering, 2005
Texas A&M University
College Station, Texas

B.S., Chemical Engineering, 1987
Amirkabir University of Technology
Tehran, Iran

Work Experience: Senior Gas Process Engineer, 1988-1998
National Iranian Oil Company
Ahwaz, Iran